





# **Interaction of Cibacron Blue Attached Magnetic Polymers with Albumin Using Computational Tools**

## **Cibacron Blue F3GA Baęlı Manyetik Polimerler ile Albumin Etkileşiminin Bilgisayarlı Ortamda İncelenmesi**

**SEÇKİN KILIÇ**

**PROF. DR. ADİL DENİZLİ**

**Supervisor**

Submitted to

Graduate School of Science and Engineering of Hacettepe University

as a Partial Fulfillment to the Requirements

for the Award of the Degree of Master of Science in Chemistry.

2019



This work titled “**Interaction of Cibacron Blue Attached Magnetic Polymers with Albumin Using Computational Tools**” by **SEÇKİN KILIÇ** has been approved as a thesis for the Degree of **Master of Science in Chemistry** by the Examining Committee Members mentioned below.

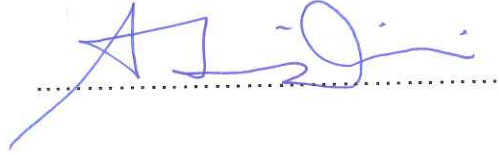
Prof. Dr. Handan YAVUZ ALAGÖZ

Head

  
.....

Prof. Dr. Adil DENİZLİ

Supervisor

  
.....

Assoc. Prof. Dr. Nilay BERELİ

Member

  
.....

Assoc. Prof. Dr. Fatma YILMAZ

Member

  
.....

Asst. Prof. Dr. Ceren HAKTANIR

Member

  
.....

This thesis has been approved as a thesis for the Degree of **Master of Science in Chemistry** by Board of Directors of the Institute of Graduate School of Science and Engineering on ..... / ..... / .....

Prof. Dr. Menemşe GÜMÜŞDERELİOĞLU

Fen Bilimleri Enstitüsü Müdürü



## ETHICS

In this thesis study, prepared in accordance with the spelling rules of Institute of Graduate School of Science and Engineering of Hacettepe University,

I declare that,

- all the information and documents have been obtained in the base of the academic rules,
- all audio-visual and written information and results have been presented according to the rules of scientific ethics,
- in case of using other works, related studies have been cited in accordance with the scientific standards,
- all cited studies have been fully referenced,
- I did not do any distortion in the data set,
- and any part of this thesis has not been presented as another thesis study at this or any other university.

21 / 06 / 2019

  
SEÇKİN KILIÇ





## YAYINLANMA FİKRİ MÜLKİYET HAKLARI BEYANI

Enstitü tarafından onaylanan lisansüstü tezimin tamamını veya herhangi bir kısmını, basılı (kağıt) ve elektronik formatta arşivleme ve aşağıda verilen koşullarla kullanıma açma iznini Hacettepe Üniversitesi'ne verdiğimi bildiririm. Bu izinle Üniversiteye verilen kullanım hakları dışındaki tüm fikri mülkiyet haklarım bende kalacak, tezimin tamamının ya da bir bölümünün gelecekteki çalışmalarda (makale, kitap, lisans ve patent vb.) kullanım hakları bana ait olacaktır.

Tezin kendi orijinal çalışmam olduğunu, başkalarının haklarını ihlal etmediğimi ve tezimin tek yetkili sahibi olduğumu beyan ve taahhüt ederim. Tezimde yer alan telif hakkı bulunan ve sahiplerinden yazılı izin alınarak kullanması zorunlu metinlerin yazılı izin alarak kullandığımı ve istenildiğinde suretlerini üniversiteye teslim etmeyi taahhüt ederim.

Yükseköğretim Kurulu tarafından yayınlanan "**Lisansüstü Tezlerin Elektronik Ortamda Toplanması, Düzenlenmesi ve Erişime Açılmasına İlişkin Yönerge**" kapsamında tezim aşağıda belirtilen koşullar haricince YÖK Ulusal Tez Merkezi / H.Ü. Kütüphaneleri Açık Erişim Sistemi'nde erişime açılır.

- Enstitü yönetim kurulu kararı ile tezimin erişime açılması mezuniyet tarihimden itibaren 2 yıl ertelenmiştir.
- Enstitü yönetim kurulu gerekçeli kararı ile tezimin erişime açılması mezuniyet tarihimden itibaren .... ay ertelenmiştir.
- Tezim ile ilgili gizlilik kararı verilmiştir.

21 / 06 / 2019

  
SEÇKİN KILIÇ



## **ABSTRACT**

### **Interaction of Cibacron Blue F3GA Attached Magnetic Polymers with Albumin Using Computational Tools**

**Seçkin KILIÇ**

**Master of Science, Department of Chemistry**

**Supervisor: Prof. Dr. Adil DENİZLİ**

**June 2019, 84 pages**

Human plasma contains a vast amount of human serum albumin (HSA). Almost 60% of human plasma protein contains HSA. Blood volume regulation based on colloid osmotic pressure is a vital role of serum albumins. In order to hide their hydrophobic nature, they can be seen transferring some low water-soluble molecules. These molecules consisted of some steroid hormones, some salts, free fatty acids, calcium, and some drugs. Low or high level of albumin almost always caused several diseases. Besides, albumin should be removed from blood plasma in some cases, since high abundancy of albumin hinders biomarkers in proteome studies. Affinity chromatography is a standard method, which used for protein purification and separation studies due to its specificity, selectivity. There are several affinity chromatography methods, such as dye affinity, immobilized metal chelated affinity, and affinity electrophoresis. Cibacron Blue F3GA (CBD), as a dye ligand, is one of the most used dyes amongst dye affinity chromatography. CBD is ideally suited for HSA purification for several years. However, even though CBD has many purification applications, there is not much research focused on the

interaction between CBD and HSA in molecular simulation. In this thesis, interactions between CBD and HSA were simulated via AutoDock molecular docking software in this study. Investigated possibilities resulted in six different conformations on different locations, which light the way to variable connectivity of CBD. Thus, it is determined that the most favorable binding is conformation 5, with its lowest binding energy, which is energetically favorable.

**Keywords:** Cibacron Blue, Human Serum Albumin, Molecular Docking, AutoDock Software

## ÖZET

### **Cibacron Blue F3GA Bağlı Manyetik Polimerler ile Albumin Etkileşiminin Bilgisayarlı Ortamda İncelenmesi**

**Seçkin KILIÇ**

**Yüksek Lisans, Kimya Bölümü**

**Tez Danışmanı: Prof. Dr. Adil DENİZLİ**

**Haziran 2019, 84 sayfa**

İnsan serumu albümini (HSA), insan plazması içeriğinde en sık karşılaşılan proteindir. Bu haliyle kan içeriğindeki proteinlerinin %60'ını oluşturur. Yağ asitleri ve ilaç gibi farklı molekülleri kan içinde aktarmasının yanında en önemli görevlerinden biri, kan ile doku sıvıları arasında su miktarının dengelenmesini, yani ozmotik basıncı sağlamaktır. Albüminin eksikliği çeşitli metabolik hastalıklara yol açmakla birlikte, kanda bol miktarda bulunması da proteom analizlerinin kısıtlanmasına neden olmaktadır. Bu nedenlerle, albümin uzun yıllardır çeşitli yöntemlerle saflaştırılmakta veya kan ortamından uzaklaştırılmaktadır. Saflaştırma ve ayırma yöntemleri arasında en sıklıkla kullanılan yöntem afinite kromatografisidir. Afinite kromatografisi, belli bir moleküler yapıya ve yönlenmeye sahip immobilize ligand ve hedef molekül arasındaki seçici, spesifik ve tersinir etkileşimlere dayanan bir ayırma yöntemidir. Afinite kromatografisi, immobilize metal şelat afinite yöntemlerinden boya afinite kromatografisi, afinite kapiler elektroforez afinite çöktürme ve afinite membranlara kadar birçok alanda kullanılan yöntemlerin başında gelmektedir. Boyar madde Cibacron Blue (CBD) ise boya

afinite kromatografisinde en çok kullanılan boya ligandlardan birisidir. HSA saflaştırılması için CBD çok uyumlu bir boya liganddır. Ancak, CBD boya ligand içeren birçok afinite uygulaması olmasına rağmen, CBD ve HSA arasındaki etkileşimin bilgisayarlı ortamda incelendiği çok fazla araştırma bulunmamaktadır. Bu kapsamdaki tez çalışmasında, CBD ve HSA arasındaki etkileşimin değerlendirilmesi için moleküler kenetlenme yazılımı AutoDock kullanılmıştır. CBD ile yapılan moleküler kenetlenme çalışmaları, altı farklı konformasyonda CBD ve HSA arasında bir etkileşim olabileceğini ve HSA'nın farklı bağlanma bölgelerine ulaşabileceğini göstermiştir. Altı farklı konformasyonun bağlanma serbest enerjileri hesaplanmıştır. CBD'nin en uygun konformasyonunda ve enerjetik olarak en istenir sonuç, konformasyon 5 için belirlenmiştir.

**Anahtar Kelimeler:** Cibacron Blue, Human Serum Albumin, Moleküler Bağlanma, AutoDock Yazılımı

## ACKNOWLEDGEMENT

It was my honor to work with Dr. Adil DENİZLİ in this thesis as my supervisor as well as Dr. A. Müge ANDAÇ ÖZDİL. Their knowledge and guidance paved the way for the foundation for my research and bred new branches for new ideas and future projects. I want to thank them profoundly for their insight, continuous support, unparalleled patience.

It is their inspiration and encouragement towards me that led me the way that I follow. As Isaac Newton said in 1676, "If I have seen further, it is by standing on ye shoulders of Giants." They become the beacon that I follow in this scientific journey.

I must express my heartfelt gratitude to my mother; with her generous support I overcome the obstacles in my life, and if my father processed his umwelt like in his old days, I believe that he would be proud as well.

Lastly, as in the words of Mustafa Kemal ATATÜRK, "Science is the most real guide for civilisation, for life, for success in the world. To search for a guide other than science is absurdity, ignorance and heresy."

Thank you all; unmentioned friends, colleagues, scientists for being in my life.





# INDEX

|   |      |
|---|------|
| ABSTRACT.....   | i    |
| ACKNOWLEDGEMENT .....   | v    |
| INDEX .....   | vii  |
| FIGURES INDEX.....  | ix   |
| TABLES INDEX .....  | xi   |
| SYMBOLS & ABBREVIATIONS .....   | xiii |
| 1.INTRODUCTION .....  | 1    |
| 2.GENERAL INFORMATION.....  | 3    |
| 2.1.Albumin .....   | 3    |
| 2.2.Dye-Ligand Affinity Chromatography.....                                 | 4    |
| 2.3.Magnetic Affinity Separation .....                                      | 5    |
| 2.3.1.Materials and Apparatus .....   | 7    |
| 2.3.2.Magnetic Affinity Separation of Proteins .....                        | 8    |
| 2.4.Computational Approach to Affinity Interactions in Chromatography ..... | 23   |
| 2.4.1.Molecular Modeling and Molecular Docking .....                        | 23   |
| 2.4.2.Importance of Using Computational Simulation.....                     | 25   |
| 2.4.3.Applications of Molecular Docking.....                                | 26   |
| 2.5.Software .....  | 26   |
| 2.5.1.AutoDock and AutoGrid .....   | 26   |
| 2.5.2.UCSF Chimera.....   | 27   |
| 2.5.3.Amber .....   | 27   |
| 2.5.4.Antechamber .....   | 28   |
| 2.5.5.MMTK .....  | 28   |
| 2.6.Molecules .....   | 28   |
| 2.6.1.Human Serum Albumin (HSA) .....                                       | 28   |
| 2.6.2.Cibacron Blue (CBD) .....   | 30   |
| 3.EXPERIMENT .....  | 33   |
| 3.1.Hardware and Operating Systems .....                                    | 33   |

|   |    |
|---|----|
| 3.2. Softwares .....  | 33 |
| 3.3. Preparation of Macromolecules.....   | 34 |
| 3.3.1. Structures from the PDB.....   | 34 |
| 3.4. Minimization and Dock Preparation.....                                     | 36 |
| 3.4.1. Targeting Binding Sites .....  | 37 |
| 4. RESULT AND DISCUSSION .....  | 39 |
| 4.1. Results .....  | 39 |
| 4.1.1. Conformation 1 .....   | 39 |
| 4.1.2. Conformation 2 .....   | 42 |
| 4.1.3. Conformation 3 .....   | 44 |
| 4.1.4. Conformation 4 .....   | 47 |
| 4.1.5. Conformation 5 .....   | 49 |
| 4.1.6. Conformation 6 .....   | 51 |
| 4.2. DISCUSSION .....   | 55 |
| 4.2.1. Binding Affinity of CBD to Human Serum Albumin (HSA).....                | 55 |
| 4.2.2. Binding Properties of CBD docked to HSA for Conf #1 and Conf #2.....     | 56 |
| 4.2.3. Binding Properties of CBD docked to HSA for Conf #3, #4, #5 and #6 ..... | 58 |
| 5. CONCLUSION.....  | 65 |
| 6. REFERENCES .....   | 67 |
| APPENDIX .....  | 81 |
| APPENDIX 1 - Originality Report .....   | 81 |
| Curriculum vitae .....  | 83 |

## FIGURES INDEX

|  |    |
|--|----|
| Figure 2.1. Three major domains accompanied by a disulfide-bonded alpha-helical subdomain of HSA are shown in the three-ball model [3].  | 4  |
| Figure 2.2. Elements in molecular docking. In this example; protein is HSA and ligand is CBD.  | 24 |
| Figure 2.3. HSA ribbon structure.  | 29 |
| Figure 2.4. The crystal structure of HSA showing drug binding sites.   | 30 |
| Figure 2.5. Cibacron Blue structure showing elements.  | 31 |
| Figure 3.1. Cibacron Blue structure, minimized and prepared for docking.   | 35 |
| Figure 3.2. Cibacron Blue structure showing active regions [139].  | 35 |
| Figure 3.3. HSA structure, minimized, and prepared for docking.  | 36 |
| Figure 3.4. Docking of CBD on HSA.   | 38 |
| Figure 4.1. A) Conformation 1, B) Conformation 2, C) Conformation 1 and 2 of CBD interaction with HSA (solid grey surface).  | 56 |
| Figure 4.2. A) Conformation 1 and B) Conformation 2 of CBD interaction with HSA interactive hydrophobicity solid surface. (Dodger blue denotes more hydrophilic surface and orange denotes more hydrophobic surface.)  | 57 |
| Figure 4.3. Conf 3, 4, 5, and 6 of CBD interaction with HSA (solid grey surface).  | 58 |
| Figure 4.4. A1) Conformation 3 of CBD interaction with HSA (interactive hydrophobicity of solid surface). A2) Conformation 3 of CBD interaction with HSA (dark grey solid surface). B) Conformation 4 of CBD interaction with HSA (dark grey solid surface). | 60 |
| Figure 4.5. A) Conformation 5 and 6 of CBD interaction with HSA (interactive hydrophobicity of surface). B) Conformation 5 and 6 of CBD interaction with HSA (dark grey solid surface).  | 62 |
| Figure 4.6. A and B) H-bonding of Conf #5 of CBD interacts with HSA (ribbon structure) in different views.   | 63 |

Figure 4.7. Interaction of Conf #5 of CBD with neighboring amino acid residues of HSA. ....64

## TABLES INDEX

|  |    |
|--|----|
| Table 2.1. List of advantages of reactive dyes [11]. .....   | 5  |
| Table 2.2. Examples of enzymes purified with magnetically responsive materials bearing natural or synthetic enzyme inhibitors..... | 10 |
| Table 2.3. Examples of enzymes purified with magnetically responsive materials bearing reactive dyes. ....                         | 13 |
| Table 2.4. Examples of enzymes purified with magnetically responsive materials bearing specific affinity ligands. ....             | 14 |
| Table 2.5. Examples of enzymes purified by magnetically modified polysaccharides. ....   | 17 |
| Table 2.6. Examples of recombinant enzymes purified with specifically designed magnetically responsive materials. ....             | 19 |
| Table 2.7. Purified enzymes using molecularly imprinted polymers.....  | 21 |
| Table 4.1. Clustering Histogram data for Conformation 1 .....  | 40 |
| Table 4.2. RMSD Values and Binding Energies of each run on Conformation 1. ..  | 40 |
| Table 4.3. Data for Lowest Energy Docking of Conformation 1 .....  | 41 |
| Table 4.4. Clustering Histogram data for Conformation 2 .....  | 42 |
| Table 4.5. RMSD Values and Binding Energies of each run on Conformation 2. ..  | 43 |
| Table 4.6. Data for Lowest Energy Docking of Conformation 2 .....  | 44 |
| Table 4.7. Clustering Histogram data for Conformation 3 .....  | 45 |
| Table 4.8. RMSD Values and Binding Energies of each run on Conformation 3. ..  | 45 |
| Table 4.9. Data for Lowest Energy Docking of Conformation 3 .....  | 46 |
| Table 4.10. Clustering Histogram data for Conformation 4. ....   | 47 |
| Table 4.11. RMSD Values and Binding Energies of each run on Conformation 4. ..   | 48 |
| Table 4.12. Data for Lowest Energy Docking of Conformation 4 .....   | 49 |
| Table 4.13. Clustering Histogram data for Conformation 5. ....   | 50 |
| Table 4.14. RMSD Values and Binding Energies of each run on Conformation 5. ..   | 50 |

|   |    |
|---|----|
| Table 4.15. Data for Lowest Energy Docking of Conformation 5 .....                      | 51 |
| Table 4.16. Clustering Histogram data for Conformation 6. ....                          | 52 |
| Table 4.17. RMSD Values and Binding Energies of each run on Conformation 6. ....        | 53 |
| Table 4.18. Data for Lowest Energy Docking of Conformation 6 .....                      | 54 |
| Table 4.19. Conformation features and binding free energies of CBD bound to<br>HSA..... | 55 |
| Table 4.20. Summary of binding features of CBD to HSA. ....                             | 65 |

## SYMBOLS & ABBREVIATIONS

### Abbreviations

|          |   |
|----------|---|
| BS1      | Binding Site 1 of HSA                   |
| BS2      | Binding Site 2 of HSA                   |
| BS3      | Binding Site 3 of HSA                   |
| CBD      | Cibacron Blue F3GA                      |
| HSA      | Human Serum Albumin                     |
| PDB      | Protein Data Bank                       |
| GUI      | Graphical User Interface                |
| MMTK     | The Molecular Modeling Toolkit          |
| UCSF     | University of California, San Francisco |
| MD       | Molecular Dynamics                      |
| MM       | Molecular Mechanics                     |
| ADT      | AutoDockTools                           |
| GA       | Genetic Algorithm                       |
| Min      | Minimization command                    |
| DockPrep | Dock preparation command                |
| LBE      | Lowest Binding Energy                   |
| MBE      | Mean Binding Energy                     |
| Conf     | Conformation                            |
| 3D       | Three-dimensional                       |





## 1.INTRODUCTION

Human plasma contains a vast amount of human serum albumin (HSA). Almost 60% of human plasma protein contains HSA. Blood volume regulation based on colloid osmotic pressure is a vital role of serum albumins. In order to hide their hydrophobic nature, they can be seen transferring some low water-soluble molecules. These molecules consisted of some steroid hormones, some salts, free fatty acids, calcium, and some drugs. Hence there is rivalry amongst drugs for albumin binding sites. This situation affects the strength of the binding process. Low or high level of albumin almost always caused several diseases. Besides, albumin should be removed from blood plasma in some cases, since high abundancy of albumin hinders biomarkers in proteome studies.

A standard method for protein purification and separation studies is affinity chromatography due to its specificity, selectivity. There are several affinity chromatography methods, such as dye affinity, immobilized metal chelated affinity, and affinity electrophoresis. Among these, dye ligand affinity chromatography is one of the most common methods for protein purifications since it binds to macromolecules to be explicitly separated and reversibly. For a feasible scenario for HSA purification, Cibacron Blue F3GA is a relatively more available dye, which was an adsorbent built upon a sulfonated triazine structure of a dye, also usable in low purity conditions. Although CBD has many albumin purification applications, there is not much research focused on identifying the molecular interaction between CBD and HSA in molecular simulation.

Computational techniques strengthen their position because they are offering such results beyond experimental possibilities for areas such as functional site location, comparative modeling, binding site recognition in proteins, protein-ligand docking as well as protein-protein docking, and molecular dynamic.

Molecular docking is basically a method based on the journey to a stable complex via interaction of two or more molecules. Such complex's 3D structure can be computed with the usage of algorithms via binding properties of ligand and protein. The ability of interaction of such protein with small molecules is crucial in which

resultant dynamics could change for the favor of enhancement or inhibition of its biological function.

In this thesis, AutoDock v4.2.6 was used for docking ligands to identify active locations for specific targeting of binding sites on target proteins. UCSF Chimera software was used for minimization of structures then preparation for docking. This process minimizes the energy of molecule models. In order for the process to succeed, some atoms could be held fixed. For the source of the protein structure, ProteinDataBank (PDB) was used via UCSF Chimera. All conformations of CBD had a 10 run of GA with 150 as population size and 27000 maximum number of generations.

## 2.GENERAL INFORMATION

### 2.1.Albumin

Distinct properties of albumin, which was not a well-known protein at the time, recognized by Professor Ansell in 1839, had essential bodily purposes. In the Lancet he said, "albumen is doubtless one of the most important of the animal proximate principles; it is found not only in the serum of the blood but in lymph and chyle, in the exhalations from serous surfaces, in the fluid of cellular tissue, in the aqueous and vitreous humours of the eye, in many other animal fluids, albumin acts sometimes as an acid and a base and its powers of maintaining its combinations is so great albumin proportions are pretty nearly the same in all higher animals, the levels are nearly the same in the sexes and between the ages of 20 and 80". Therefore, for over 180 years, we have become known of some highly accurate description of serum albumin properties [1].

HSA has a single, polypeptide chain, which is non-glycosylated, containing amino acid residues with a total of 585. It has an amino-acid order which incorporates 17 disulfide bridges, consisting of Cys 34 and Trp 214. The other structural distinction of HSA is a unique pattern of double ribbons. Disulfide bridges hold jointly said loops [2]. HSA incorporates electrostatically different three massive domains, charge-pH properties, and denaturability. Figure 2.1 illustrates the three-ball and a container shape with amino acid order folding pattern and size of HSA [3]. There are three domains called DI for Domain I, DII for Domain II, and DIII for Domain III can be seen in Figure 2.1 from N terminal to C terminal, from left to right respectively. Each domain has its merits. Domain III has two high-affinity attachment sites mainly for fatty acid. However, Domain I and Domain II has central sites. Both situations remarkably increase conformational stability [3].

Human plasma contains a vast amount of HSA. Almost 60% of human plasma proteins consist of HSA. If immunoglobulin was counted, the total amount jumps to 80%. HSA can be found in tissues and some other parts in the body. HSA has a wide variety of physiological functions. Furthermore, it contributes significantly to colloid osmotic blood pressure in-vivo. Plus, HSA can be used to convey and

allocate many chemically diverse substances [4]. Those molecules have a very wide range of possibilities. Such as amino acids like cysteine, tryptophan, and tyrosine; bile acids, bilirubin, and long-chain fatty acids and hormones like aldosterone, cortisol, and testosterone are also among those substances. Accordingly, one must add metal ions like copper, calcium, chloride, magnesium, zinc, and several pharmaceuticals to the list as well [5].

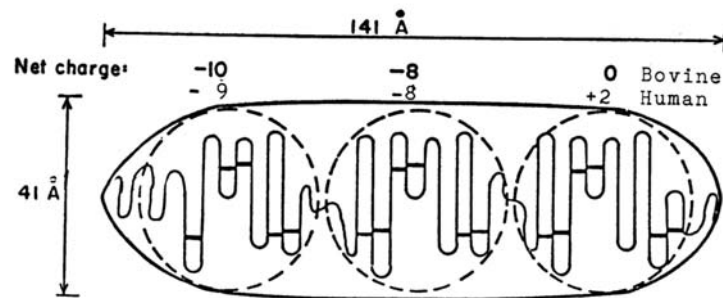


Figure 2.1. Three major domains accompanied by a disulfide-bonded alpha-helical subdomain of HSA are shown in the three-ball model [3].

## 2.2. Dye-Ligand Affinity Chromatography

In order to acquire purified proteins, there are several techniques to choose on. Yet dye-ligand affinity chromatography is increasingly valuable and a comparatively advantageous technique [6]. Table 2.1 shows some of the advantages. The triazine scaffold containing dyes have specific binding abilities [7-9]. Although all dyes are synthetic their classification of pseudo-specific affinity ligands doesn't change. In particular such dyes use mimicry while binding to proteins [10].

In contrast, commercially available dyes are not well equipped for usage right away; instead, they tend to have some various impurities which needed to be purified via chromatographic techniques [12, 13]. However, those techniques are necessary, only when immobilized dyes are used. Consequently, a small number of contaminants would be immobilized on the matrix, and they would be gone after washing [14-16].

Table 2.1. List of advantages of reactive dyes [11].

---

Economically and universally accessible  
Immobilization efficiency  
Avoids hazardous and toxic reagents in matrix activation  
Stable against biological and chemical attack  
Storage of matrix without activity loss  
Reusable, withstand cleaning and sterilization  
Ease of scaling  
High capacity  
Medium specificity

---

### **2.3.Magnetic Affinity Separation**

Isolation and purification of enzymes from various biological sources is a crucial part of enzymology. Protein purification process generally a four-stage process, namely; recovery, concentration, purification, and formulation; hence, each have different objectives. Study of separation procedures enabling to obtain pure or substantially purified enzymes is significant. Production costs of proteins is a setback in some cases because they tend to carve out 30 – 80% of costs alone [17]. Advanced separation techniques are a necessity. Such techniques should be capable of treating solutions containing target enzyme(s) regardless of some small impurities and in the presence of large quantities of accompanying proteins and other low and high molecular weight compounds via both comprehensive and straightforward processes.

In biochemistry and biotechnology, target enzymes isolation is customarily carried out using all sorts of techniques like chromatography, electrophoretic, ultrafiltration, precipitation [18]. Among them, affinity chromatography is one of the most vital technique; which has a vast amount of successful laboratory scale applications in its inventory. Nonetheless, the main drawback of standard column affinity chromatography is the impossibility to handle samples containing

contaminating particulate material. Affinity chromatography does not work with contaminated materials or materials that have not already been purified. For these kinds of purposes, if a successful result is desired, a batch separation process for magnetic affinity adsorption can be used.

Magnetic separations represent extremely versatile separation processes enabling to isolate and purify peptides, proteins, nucleic acids, cells, viruses, environmental contaminants, and other target molecules directly from crude samples. Batch magnetic affinity separation of target enzymes can be performed straightforwardly and rapidly, with not many handling steps. The whole process of the enzyme purification method can be performed in a single test tube. Immobilized affinity ligand carrying magnetic carriers as well as magnetically responsive biopolymer particles having an affinity for the isolated enzyme or specifically designed magnetic molecularly imprinted polymer particles are mixed with an appropriate enzyme source. The separation process, which is usually very gentle to the target enzyme(s), can be carried out straight in impure samples. Such impurities have suspended solid material. Column chromatography techniques have the ability to broke up big protein complexes if magnetic separation techniques have been carefully established. Magnetic techniques can also be used for enzyme concentration from diluted solutions. In connection to magnetic properties of magnetic adsorbent substances, they can be selectively separated from such sample comparatively with ease. Whole blood, plasma, urine, milk, whey, food waste, and numerous other materials can be used to isolate target enzymes. However, the binding process does not occur right away. There is an incubation period to think of. Finally, magnetic particles and targets are bound after such a process. A magnetic separator is all that is needed for the removal of the complex with ease [19,20]. In addition to laboratory scale separations, these techniques can also find applications in larger-scale processes [21,22]. Several alternative approaches, such as separation in fluidized beds, which are already magnetically stabilized [17,23], or magnetic two-phase systems [24] were described.

Typical examples of published purification procedures document the effectiveness of magnetic affinity separation techniques. Recently published review papers on similar topic present up-to-date applications of magnetic separation procedures

and document continuing the importance of this experimental approach [17,25-29].

### **2.3.1. Materials and Apparatus**

It is a straightforward process to use magnetic separators and do experiments. Rare-earth magnets such as NdFeB are the go-to choice for magnetic separators since they are widely available from a variety of sources worldwide. Commercial laboratory scale separators have disinfectant-proof materials as a difference from their consumer counterparts. On the other hand, racks have to accommodate different types of vessels. In order to separate larger volumes such as 500 – 1000 mL, flat ones are more appropriate.

Large volume magnetic separation systems for bottles of different volumes can be successfully used for both batch and flow-through magnetic separations [30]. A review paper put on word for separating magnetic particles with a diameter of ca 1  $\mu\text{m}$  or larger [19]. Separation of nanoparticles and sub-micrometer sized particles possibly necessitate the involvement of other separators. Such need can be overcome with the usage of high gradient magnetic separators use steel balls or wool-packed columns. Columns later separated from the magnetic field, in order to particles to be retained in the matrix. A gentle vibration is nice to have [19,31].

Appropriate magnetically responsive affinity materials are used to capture the target enzyme from its source. Commercial [17,29] or laboratory prepared [29,32] magnetic materials are available in the market. That kind of materials can be seen in the market as magnetic particles. Such particles have been produced from various synthetic polymers (e.g., polystyrene), biopolymers (e.g., cellulose, chitin, chitosan, dextran), porous glass, or silica. Alternatively, such particles could be based on surface-modified (silanized) iron oxide (magnetite, maghemite, or ferrites) can be used. Magnetic particles usually carry appropriate functional groups (e.g., amino, carboxyl or thiol ones), which enable subsequent affinity ligand immobilization. Besides, activated magnetic particles are already obtainable from the market, which in turn enable direct binding of affinity ligands.

The breadth of magnetic particles mostly differs from ca 50 nm to approximately 10  $\mu\text{m}$  [17, 19,33]. Nevertheless, millimeter range diameter having particles are

not impossible either [34]. Ideal properties of a magnetic adsorbent good enough for bioseparation proposes to comprehend a high binding capacity, low non-specific binding, and physicochemical robustness [29].

### **2.3.2. Magnetic Affinity Separation of Proteins**

One of the two mainly used methods for magnetic affinity separation is the direct method. In this direct method, magnetic affinity adsorbent is added to the sample, which causes a tendency for binding of target compounds. Another method is the indirect method. However, in this method, the sample is being added a free affinity ligand. This action makes it possible for the target compound to interact with the ligand. As a result, magnetic particles catch the final complex. In both methods, magnetically separated and washed particles have been used, and then the target compounds are eluted. If ligands and the target do not have high affinity, the indirect method can also be used [19].

As stated above, magnetic affinity separation of enzymes is usually based on the interaction of the target enzyme(s) with an appropriate affinity ligand bound to the magnetic carrier. Useful inspiration for how to find an appropriate affinity ligand-target enzyme combination can be found in standard affinity chromatography. Typical affinity ligands comprehend natural and synthetic enzyme inhibitors (Table 2.2), reactive organic dyes (Table 2.3) and many other molecules such as substrates, antibodies, affitins, aptamers, chelated heavy metal ions, synthetic peptides, amino acids, drugs and some others (Table 2.4). Many procedures are available for binding the specific affinity ligand to an appropriate magnetic carrier; e.g., magnetic supports bearing amino groups can be easily activated by glutaraldehyde to enable binding of amino groups containing molecules. Alternatively, magnetically modified biopolymers such as chitin, chitosan, starch, alginate, or lignocellulose can be used for the same purpose (Table 2.5). A simple magnetic modification of affinity adsorbents used for standard affinity chromatography (e.g., by magnetic fluids) can be employed for magnetic affinity adsorbents preparation [35]. For large scale purification processes usually cost-effective and robust synthetic affinity ligands including synthetic triazine dyes like CBD are predominantly used due to their particularly selective behavior for binding



with most proteins. Triazine dyes also show resistance to chemical and biological degradation.

Recently the production of recombinant proteins in a highly purified and well-characterized form has become an important task. The fusion proteins contain an appropriate affinity tag structure enabling single-step adsorption purification with a very little effect on the tertiary structure and biological activity and its smooth and distinct removal to help produce the native protein. Fusion tags with different sizes and biochemical properties have been constructed with respectable quantities; depending on their applications and biochemical properties, fusion tags are categorized into a number of groups (which may overlap with each other), including affinity fusion tags, fluorescence protein tags, enzyme tags, protein tags, peptide tags and epitope tags [36]. The most often used histidine-tagged (His-tag) proteins are usually magnetically separated with the particles having nitrilotriacetic acid or  $N\alpha, N\alpha$ -Bis(carboxymethyl)-L-lysine hydrate ligands loaded with nickel or cobalt ions [25]. Typical examples of successful magnetic separation of recombinant enzymes are presented in Table 2.6.

In order to generate specific binding sites, one could use molecular imprinting as a way of achieving effectiveness. With this method, highly specified molecularly imprinted polymers (MIP) can be acquired. This type of process is highly advantageous to the natural process of generating receptors like antibodies. To date, different kinds of MIPs have been successfully developed for the separation of small molecules. On the other hand, MIP preparation for biomacromolecules, including enzymes, is not an easy task; entrapment of protein molecules in a polymer network and their subsequent removal is a problematic step [37]. Currently, mainly lysozyme is used as the enzyme template for the construction of magnetically responsive molecularly imprinted polymers; typical examples of lysozyme separation are presented in Table 2.7.

As shown in Tables 2.2 to 2.7, magnetic affinity separations of target enzymes have been successfully presented in many various papers. There is no simple strategy to isolate target enzymes; various approaches have been tested to obtain a purified enzyme. The data in the following tables can serve as an inspiration for

a broad scientific and technological community with the possibility to implement magnetic technologies into their experimental work in order to improve the conventional procedures.

Table 2.2. Examples of enzymes purified with magnetically responsive materials bearing natural or synthetic enzyme inhibitors.

| <b>Enzyme (Purified)</b>  | <b>Main Source</b>                      | <b>Magnetic carrier</b>                  | <b>Inhibitor</b>   | <b>Additional details</b>  | <b>References</b> |
|---------------------------|---|--|--|--|-------------------|
| Aminopeptidase            | <i>Arabidopsis</i>                      | Amine-terminated magnetic beads          | N-1-Naphthylphthalamic acid                              | KCl gradient elution   | [38]              |
| Gastric aspartic protease | Rat gastric mucosa                      | Magnetic glyoxal 4% agarose beads        | Synthetic heptapeptides containing D-amino acid residues | Elution with acetate and phosphate buffers containing 20% 2-propanol | [39]              |
| Nattokinase               | <i>Bacillus natto</i>                   | Magnetic poly(methyl methacrylate) beads | p-Aminobenzamide   | Eluted by 0.1 M ammonium acetate buffer (pH 4.0)                     | [40]              |
| Pepsin                    | Human gastric juice, rat gastric mucosa | Magnetic glyoxal agarose beads           | Synthetic heptapeptide containing D-amino acid residues  | Eluted by 20% acetonitrile in 0.1 M acetate buffer (pH 3.5)          | [41]              |

| <b>Enzyme (Purified)</b> | <b>Main Source</b>            | <b>Magnetic carrier</b>  | <b>Inhibitor</b>   | <b>Additional details</b>                                   | <b>References</b> |
|--------------------------|-------------------------------|--|--------------------|---|-------------------|
| Protease (Savinase)      | <i>Bacillus clausii</i>       | Silanized magnetite nanoparticles                                | Bacitracin         | High gradient magnetic separation used                      | [42]              |
| Protease                 | <i>Bacillus licheniformis</i> | Silanized magnetite particles                                    | Bacitracin         | Semi-continuous <i>in situ</i> magnetic separation used     | [43]              |
| Protease                 | <i>Bacillus licheniformis</i> | Silanized magnetite particles                                    | Bacitracin         | High gradient fishing used                                  | [44]              |
| Subtilisin               | Commercial preparation        | Magnetic carrier bearing epoxy groups                            | Benzamidine        | Elution at pH 6 (0.1 M of glycine-HCl buffer)               | [45]              |
| Trypsin                  | Porcine pancreatin            | Silanized magnetic particles                                     | Benzamidine        | High gradient magnetic separation                           | [31]              |
| Trypsin                  | Bovine pancreas               | Magnetic poly(glycidyl methacrylate-co-methylmethacrylate) beads | p-Aminobenzamidine | Separation in magnetically stabilized fluidized bed reactor | [23]              |

| <b>Enzyme (Purified)</b> | <b>Main Source</b>     | <b>Magnetic carrier</b>                   | <b>Inhibitor</b>          | <b>Additional details</b>   | <b>References</b> |
|--------------------------|------------------------|---|---------------------------|---|-------------------|
| Trypsin                  | Commercial preparation | Magnetite and magnetic chitosan particles | Soybean trypsin inhibitor | Batch stirred tank, and magnetically stabilized fluidized bed operations tested | [46]              |
| Trypsin                  | Commercial preparation | Submicron ferrite particles               | Soybean trypsin inhibitor | Trypsin recovered from casein solution after its hydrolysis                     | [47]              |
| Trypsin                  | Commercial preparation | Magnetic chitosan particles               | Aprotinin                 | Eluted by acetic acid including KCl solution                                    | [48]              |
| Urokinase                | Crude preparation      | Magnetic dextran microspheres             | p-Aminobenzamide          | Comparison with other affinity ligands  | [49]              |
| Urokinase                | Crude preparation      | Magnetic agarose microspheres             | p-Aminobenzamide          | Comparison with other affinity ligands  | [50]              |

Table 2.3. Examples of enzymes purified with magnetically responsive materials bearing reactive dyes.

| <b>Enzyme (Purified)</b> | <b>Main Source</b>                        | <b>Magnetic carrier</b>                          | <b>Dye</b>         | <b>Additional details</b>   | <b>References</b> |
|--------------------------|---|--|--------------------|---|-------------------|
| Alcohol dehydrogenase    | Baker's yeast homogenate                  | Magnetic cross-linked polyvinyl alcohol          | Cibacron blue F3GA | Eluted by phosphate buffer (pH 7.9) in 2 $\mu$ M 2-mercaptoethanol and 1.0 M NaCl | [51]              |
| Alcohol dehydrogenase    | <i>Saccharomyces cerevisiae</i>           | Magnetic poly(HEMA) nanoparticles                | Reactive Green 19  | Eluted by 1 M NaCl  | [52]              |
| Cellulase                | Cow's rumen fluid                         | Polymer grafted magnetic nanoparticles           | Cibacron Blue F3GA | Eluted by 1 M NaCl  | [53]              |
| Lactate dehydrogenase    | Porcine muscle                            | Magnetic agarose beads                           | Reactive Red 120   | Eluted by NaCl, gradiently  | [54]              |
| Lysozyme                 | Commercial preparation                    | Magnetic cross-linked polyvinylalcohol           | Cibacron blue 3GA  | Eluted by 1 M NaCl  | [51]              |
| Lysozyme                 | Commercial preparation, chicken egg white | Magnetic poly(2-hydroxyethyl methacrylate) beads | Cibacron Blue F3GA | Eluted by 0.1 M Tris/HCl buffer in 0.5 M NaCl                                     | [55]              |
| Lysozyme                 | Commercial preparation, chicken egg white | Magnetic chitosan microspheres                   | Reactive Red 120   | Eluted by phosphate buffer in 1M NaCl (pH 6.0)                                    | [56]              |

| <b>Enzyme (Purified)</b> | <b>Main Source</b>     | <b>Magnetic carrier</b>                          | <b>Dye</b>          | <b>Additional details</b>                                      | <b>References</b> |
|--------------------------|------------------------|--|---------------------|--|-------------------|
| Lysozyme                 | Commercial preparation | Magnetic poly(2-hydroxyethyl methacrylate) beads | Cibacron blue F3GA  | Eluted by 1.0 M KSCN (pH 8.0)                                  | [57]              |
| Lysozyme                 | Commercial preparation | Magnetic agarose beads                           | Cibacron blue 3GA   | Separation in a liquid magnetically stabilized fluidized bed   | [58]              |
| Lysozyme                 | Commercial preparation | Chitosan modified magnetic fluid                 | Cibacron Blue 3GA   | Adsorption isotherm expressed by the Langmuir adsorption model | [59]              |
| Phytase                  | Cow's rumen fluid      | Polymer grafted magnetic nanoparticles           | Cibacron blue F-3GA | Eluted by 1 M NaCl   | [60]              |

Table 2.4. Examples of enzymes purified with magnetically responsive materials bearing specific affinity ligands.

| <b>Enzyme (Purified)</b> | <b>Main Source</b> | <b>Magnetic carrier</b>  | <b>Affinity ligand</b> | <b>Additional details</b>  | <b>References</b> |
|--------------------------|--------------------|--|------------------------|--|-------------------|
| Alkaline phosphatase     | Hen's egg yolk     | Six different types of magnetic nanocarriers with varying lengths of the linkers | Arsanilic acid         | Eluted by 0.01M Tris/HCl buffer (pH 8.4) in 2.5 mM MgCl <sub>2</sub> and 20 mM Na <sub>3</sub> PO <sub>4</sub> .12H <sub>2</sub> O | [61]              |

| <b>Enzyme (Purified)</b> | <b>Main Source</b>               | <b>Magnetic carrier</b>  | <b>Affinity ligand</b>                          | <b>Additional details</b>                       | <b>References</b> |
|--------------------------|----------------------------------|--|---|---|-------------------|
| Amylase                  | <i>Tilapia</i> intestine         | Epichlorohydrin modified superparamagnetic particles                               | Soluble starch                                  | Eluted by phosphate buffer (pH 7.0) in 1 M NaCl | [62]              |
| Asparaginase             | <i>E. coli</i> homogenate        | Magnetic polyacrylamide gel particles  | D-Asparagine                                    | Eluted by D-asparagine solution                 | [63]              |
| Cellulase                | <i>Trichoderma viride</i>        | Silica modified magnetite nanoparticles  | Aminophenyl-boronic acid                        | Eluted under acidic conditions                  | [64]              |
| Dehydrofolate reductase  | HeLa cells cytoplasmic fraction  | 40 nm magnetite particles/ poly(styrene-co-glycidyl methacrylate (GMA))/ poly(GMA) | Methotrexate                                    | Eluted by SDS-PAGE loading                      | [65]              |
| Deoxycytidine kinase     | THP-1 cells cytoplasmic fraction | 40 nm magnetite particles/ poly(styrene-co-glycidyl methacrylate (GMA))/ poly(GMA) | Methotrexate                                    | Eluted by SDS-PAGE loading                      | [65]              |
| $\beta$ -Galactosidase   | <i>E. coli</i> homogenate        | Silanized magnetite  | p-Aminophenyl- $\beta$ -D-thiogalactopyranoside | Eluted by borate buffer (pH 10)                 | [63]              |

| <b>Enzyme (Purified)</b>               | <b>Main Source</b> | <b>Magnetic carrier</b>                                  | <b>Affinity ligand</b>     | <b>Additional details</b>                                 | <b>References</b> |
|--|--------------------|--|----------------------------|---|-------------------|
| Lysozyme                               | Chicken egg white  | Silica coated magnetic particles                         | Anti-lysozyme affitin      | Eluted by 100 mM glycine-HCl buffer, 0.15 M NaCl (pH 2.5) | [66]              |
| Lysozyme                               | Chicken egg white  | Magnetic poly(glycidyl methacrylate) [m-poly(GMA)] beads | L-tryptophan               | Eluted by 0.1 M methylene glycol solution                 | [67]              |
| Nattokinase                            | Natto powder       | Carboxyl modified iron oxide nanoparticles               | Arginine                   | Langmuir isotherm followed during the enzyme adsorption   | [68]              |
| Paraoxonase 1 (aryldialkylphosphatase) | Human serum        | Magnetite nanoparticles with bound p-aminohippuric acid  | Cholesterol                | Eluted by sodium deoxycholate                             | [69]              |
| Peroxidase                             | Horseradish        | Silica coated magnetite particles                        | 4-vinylphenyl-boronic acid | The particles have a high affinity for glycoenzyme        | [70]              |
| RNase B                                | Bovine             | Carboxyl-functionalized magnetic beads                   | Concanavalin A             | Elution performed under acidic conditions                 | [71]              |
| RNase B                                | Bovine             | Carboxyl-functionalized magnetic beads                   | Phenylboronic acid         | Elution performed under acidic conditions                 | [71]              |



| <b>Enzyme (Purified)</b> | <b>Main Source</b>                            | <b>Magnetic carrier</b>   | <b>Affinity ligand</b>   | <b>Additional details</b>   | <b>References</b> |
|--------------------------|---|---|--------------------------|---|-------------------|
| RNase B                  | Bovine  | Carboxyl-functionalized magnetic beads                                    | Aminophenyl-boronic acid | Bound enzyme used for (MALDI-TOF-MS).                               | [72]              |
| Subtilisin               | Commercial preparation                        | Magnetic carrier bearing epoxy groups                                     | Phenylboronic acid       | Eluted by 0.1 M ammonium acetate (pH 6) in 0.05 M MgCl <sub>2</sub> | [45]              |
| Trypsin                  | Nile tilapia ( <i>Oreochromis niloticus</i> ) | Magnetic particles coated with polyaniline, activated with glutaraldehyde | Azocasein                | Eluted by 3M NaCl   | [73]              |

Table 2.5. Examples of enzymes purified by magnetically modified polysaccharides.

| <b>Enzyme (Purified)</b> | <b>Main Source</b>                | <b>Magnetic affinity absorbent</b>           | <b>Additional details</b>                                   | <b>References</b> |
|--------------------------|-----------------------------------|--|---|-------------------|
| Amylase                  | <i>Bacillus megaterium</i>        | Starch functionalized magnetic nanoparticles | 12.5-fold purification obtained                             | [74]              |
| $\alpha$ -Amylase        | <i>Bacillus amyloliquefaciens</i> | Magnetic alginate microspheres               | 9-fold purification obtained                                | [75]              |
| $\alpha$ -Amylase        | Porcine pancreas                  | Magnetic alginate microspheres               | 12-fold purification obtained                               | [75]              |
| $\alpha$ -Amylase        | Wheat germ                        | Magnetic alginate beads                      | 1 M maltose used for elution; 48-fold purification obtained | [34]              |

| <b>Enzyme (Purified)</b>        | <b>Main Source</b>          | <b>Magnetic affinity absorbent</b>  | <b>Additional details</b>  | <b>References</b> |
|---------------------------------|-----------------------------|---|--|-------------------|
| β-Amylase                       | Sweet potato                | Magnetic alginate beads   | 1 M maltose used for elution; 37-fold purification obtained                            | [76]              |
| Chitinase                       | <i>Euphorbia characias</i>  | Chitin modified with microwave synthesized magnetic iron oxide particles          | Complex enzyme characterization  | [77]              |
| Chitinase                       | <i>Euphorbia characias</i>  | Chitin modified with microwave synthesized magnetic iron oxide particles          | Tested as a novel and powerful plant-based pesticide against <i>Drosophila suzukii</i> | [78]              |
| Cyclodextrin glucanotransferase | <i>Bacillus circulans</i>   | Magnetic porous corn starch   | CGTase recovery 60 – 70%; purification factor 19 – 25                                  | [79]              |
| Glucoamylase                    | <i>Aspergillus niger</i>    | Magnetite alginate beads  | 1 M maltose used for elution; 31-fold purification obtained                            | [76]              |
| Lysozyme                        | Hen egg white               | Magnetically modified chitin  | Comparison with magnetic agar and agarose  | [80]              |
| Lysozyme                        | Hen egg white               | Magnetically modified chitin  | The capacity was 2.5 mg of lysozyme per 1 mL of sorbent                                | [81]              |
| Lysozyme                        | Hen egg white               | Ferrofluid modified lignocellulose (spruce sawdust)                               | Eluted by 0.5 M NaCl   | [82]              |
| Lysozyme                        | <i>Ornithodoros moubata</i> | Magnetic chitin prepared from magnetic chitosan after acetic anhydride conversion | Lysozyme had a pI near 9.7 and pH optimum in the range between pH 5-7                  | [83]              |

| <b>Enzyme (Purified)</b> | <b>Main Source</b>                | <b>Magnetic affinity absorbent</b> | <b>Additional details</b>                                      | <b>References</b> |
|--------------------------|-----------------------------------|------------------------------------|--|-------------------|
| Pectinase                | <i>Aspergillus niger</i>          | Alginate magnetite beads           | Eluted by distilled water (pH 5.9) in 0.5 mM CaCl <sub>2</sub> | [84]              |
| Pullulanase              | <i>Bacillus acidopullulyticus</i> | Magnetite alginate beads           | 1 M maltose used for elution; 49-fold purification obtained    | [76]              |

Table 2.6. Examples of recombinant enzymes purified with specifically designed magnetically responsive materials.

| <b>Recombinant Enzyme (Purified)</b> | <b>Main Source</b>                   | <b>Magnetic carrier</b>  | <b>Affinity ligand</b> | <b>Additional details</b>  | <b>References</b> |
|--------------------------------------|--------------------------------------|--|------------------------|--|-------------------|
| Aldolase (histidine-tagged)          | Pea (expressed in <i>E. coli</i> )   | Magnetic kernel and nickel-silica composite matrix   | Ni <sup>2+</sup>       | Eluted by imidazole including buffer                               | [85]              |
| Arginine kinase (histidine-tagged)   | Expressed in <i>E. coli</i>          | Bifunctional Au-Fe <sub>3</sub> O <sub>4</sub> nanoparticles modified with nitrilotriacetic acid | Ni <sup>2+</sup>       | Eluted by imidazole solution                                       | [86]              |
| Carbonyl-reducing enzymes            | Human (expressed in <i>E. coli</i> ) | Commercial magnetic particles (SiMAG-NH <sub>2</sub> , SiMAG-COOH, Perloza MG)                   | Oracin                 | Eluted by buffer 0.16% NH <sub>4</sub> OH and 10% glycerol (pH 10) | [87]              |

| Recombinant Enzyme (Purified)                                | Main Source   | Magnetic carrier  | Affinity ligand      | Additional details                    | References |
|--|---|---|----------------------|---------------------------------------|------------|
| Cellulase (histidine-tagged)                                 | <i>Clostridium cellulolyticum</i> (expressed in <i>E. coli</i> )        | Fe <sub>3</sub> O <sub>4</sub> /(poly (N,N'-methylenebisacrylamide-co-glycidyl methacrylate)) microspheres bearing iminodiacetic acid | Ni <sup>2+</sup>     | Eluted by imidazole solution          | [88]       |
| CMP-Sialic acid synthetase (chitin binding domain-tagged)    | Expressed in <i>E. coli</i>   | Chitin modified magnetic nanoparticles  | Water soluble chitin | Eluted by 80 mM 1,4-dithiothreitol    | [89]       |
| Endo-β-1,4-xylanases (histidine-tagged)                      | <i>Fusarium graminearum</i> (expressed in <i>E. coli</i> )              | Ni-NTA magnetic agarose beads   | Ni <sup>2+</sup>     | Study of enzyme inhibition            | [90]       |
| Esterase (histidine-tagged)                                  | <i>Pseudomonas fluorescens</i> (expressed in <i>E. coli</i> )           | MagneHis Ni particles   | Ni <sup>2+</sup>     | Automated microscale purification     | [91]       |
| β-Glucuronidases   | <i>Penicillium purpurogenum</i> Li-3 (expressed in <i>E. coli</i> BL21) | Carboxyl modified magnetic beads  | Aptamers             | Eluted by NaCl (>330 mM)              | [92]       |
| Helper component-proteinase (maltose-binding protein-tagged) | <i>Zucchini yellow mosaic virus</i> (expressed in <i>E. coli</i> )      | Amylose magnetic beads  | Amylose              | Eluted by MPB-buffer in 10 mM maltose | [93]       |

| <b>Recombinant Enzyme (Purified)</b>          | <b>Main Source</b>   | <b>Magnetic carrier</b>  | <b>Affinity ligand</b> | <b>Additional details</b>   | <b>References</b> |
|---|--|--|------------------------|---|-------------------|
| Heparinase I (maltose-binding protein-tagged) | <i>Flavobacterium heparinum</i> (expressed in <i>E. coli</i> ) | Fe <sub>3</sub> O <sub>4</sub> @SiO <sub>2</sub> -poly(ethylene oxide)-maltose nanoparticles | Maltose                | Adsorbed enzyme used during production of low molecular weight heparins | [94]              |
| Urikase (histidine-tagged)                    | <i>Bacillus</i> (expressed in <i>E. coli</i> )                 | Ni ion-chelating magnetic beads  | Ni <sup>2+</sup>       | Eluted by cleavage with proteinase K                                    | [95]              |

Table 2.7. Purified enzymes using molecularly imprinted polymers

| <b>Enzyme (Purified)</b> | <b>Main Source</b>     | <b>Magnetic affinity absorbent</b>  | <b>Additional details</b>                       | <b>References</b> |
|--------------------------|------------------------|---|---|-------------------|
| Bromelain                | Commercial preparation | Magnetic pericarpium granati-derived carbon modified with polydopamine layer in the presence of bromelain in a weak alkaline aqueous solution | Eluted by 2% acetic acid and SDS                | [96]              |
| Lysozyme                 | Egg white              | Superparamagnetic lysozyme surface-imprinted polymer synthesized by atom transfer radical polymerization procedure                            | Eluted by PEG/sulphate aqueous two-phase system | [97]              |

| <b>Enzyme (Purified)</b> | <b>Main Source</b>     | <b>Magnetic affinity absorbent</b>  | <b>Additional details</b>                               | <b>References</b> |
|--------------------------|------------------------|---|---|-------------------|
| Lysozyme                 | Commercial (egg white) | Silica coated Fe <sub>3</sub> O <sub>4</sub> nanoparticles coated with MIP film formed from acrylamide and methacrylic acid as co-monomers  | Eluted by 0.5 M NaCl                                    | [98]              |
| Lysozyme                 | Real egg white samples | Magnetic nanoparticles coated with thermoresponsive MIP layer using (N-methacryloyl-L-alanine methyl ester) as the functional monomer and N,N'-methylenebis(acrylamide) as the crosslinker  | Eluted by altering the temperature of aqueous solution. | [20]              |
| Lysozyme                 | Commercial preparation | The imprinted polymers were coated on the surface of silica-coated magnetite nanoparticles by the surface graft copolymerization.   | Eluted by 0.5 M NaCl                                    | [99]              |
| Lysozyme                 | Commercial preparation | Core-shell magnetic chitosan submicrospheres functionalized with maleic acid and then coated with imprinted polymer layers  | Eluted by 0.5 M NaCl                                    | [100]             |
| Lysozyme                 | Egg white              | Fe <sub>3</sub> O <sub>4</sub> nanoparticles modified with 3-(methacryloyloxy)propyltrimethoxysilane and coated with a polymer film formed by the copolymerization of functional monomer acrylamide, cross-linking agent N,N'-methylenebisacrylamide, the initiator azodiisobutyronitrile, and lysozyme | Elution by 3% (v/v) acetic acid/ 10% (w/v) SDS          | [101]             |
| Lysozyme                 | Human urine            | Fe <sub>3</sub> O <sub>4</sub> nanoparticles coated with a thin film obtained using lysozyme as a template, methacrylic acid and acrylamide as functional co-monomers, and N,N'-methylenebisacrylamide as a crosslinker   | Eluted by 0.5 mM NaCl (pH 13)                           | [102]             |

## **2.4. Computational Approach to Affinity Interactions in Chromatography**

The techniques for the separation and purification of macromolecules, such as proteins and enzymes, are improving day by day. It has been an essential requirement for many of the developments made in bioscience and biotechnology over the last decades. Innovations in materials and computerized devices, with the increased use of *in vivo* tagging, have made macromolecules separation processes more predictable and controllable. Therefore, usage of such advanced techniques positively causes a time gain for researchers because they provide an adequate way to purify an enzyme or hormone from a cell extract even before the experimentation.

The fundamental basis of a variety of applications is the understanding of protein-ligand interactions. These kinds of applications cover biopharmaceutical products, innovative studies, medicinal development initiatives, biotechnology goods, molecular target verification, and large scale data analyses like high-throughput screening. In general, ligands interact with specific binding sites of macromolecular targets.

### **2.4.1. Molecular Modeling and Molecular Docking**

Molecular modeling currently is a promising field. It covers a vast amount of possibilities such as building and visualizing molecules in 3D as well as performing complex computer simulations on macromolecules of several proteins. Many software packages make it possible to do molecular modeling. Via those software packages, molecular models can be visualized, rotated, manipulated in 3D, and optimized with several algorithms. Of course, simple calculations can be performed in a few seconds while more advanced and complicated calculations possibly can take weeks or months to complete, even if a supercomputer is involved.

Computational approaches to functional site discovery, comparative modeling, characterization of ligand binding sites in protein-protein or protein-ligand docking arrangements, and molecular dynamics have become more and more significant. Even some results surpass experimental possibilities and provide guidance for

some.

Molecular docking investigates the interaction of two or more molecules, preferably protein-ligand or protein-protein, to provide a stable adduct. It is possible to calculate the 3D structure of any complex based on the interaction properties of proteins and ligands in question with the usage of different algorithms with different approaches. The behavior of this relationship can be illustrated by molecular docking (Figure 2.2).

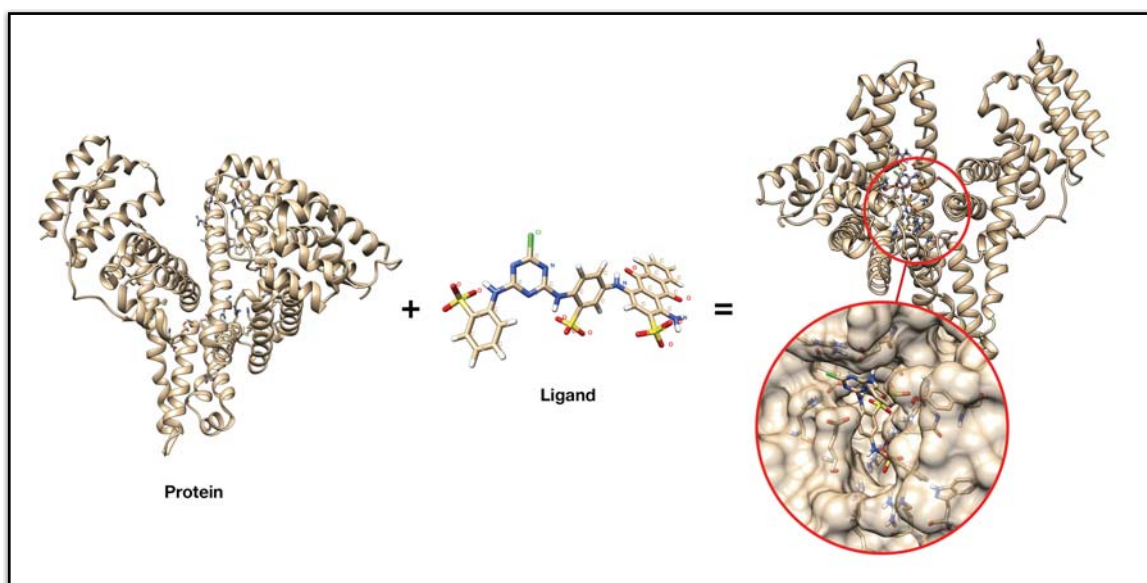


Figure 2.2. Elements in molecular docking. In this example; protein is HSA and ligand is CBD.

There are many possibilities after a molecular docking process completed, but the results are determined and ranked via many parameters using a scoring function in the software package. It is the total energy of the system with differentiating correct binding mode, gives the optimized result of the docked conformation. There are several potential paths; however, tautomerism and ionization based ligand chemistry, the single conformation of the rigid receptor calculation based on receptor flexibility, and scoring function remained the limitations.

Molecular docking is an exciting and continuously developing field which revolves around the potential activity and specificity of ligands and proteins to achieve a stable complex by determining favored binding sites of the protein for which the ligand to bind with [103,104].



The primary goal of molecular docking method is to achieve a ligand-protein adduct with optimum conformation. The net predicted  $\Delta G_{\text{bind}}$ , the binding free energy, is unveiled in terms of several parameters such as hydrogen bond ( $\Delta G_{\text{H-bond}}$ ), torsional free energy ( $\Delta G_{\text{tor}}$ ), electrostatic ( $\Delta G_{\text{elec}}$ ), desolvation ( $\Delta G_{\text{desolv}}$ ), dispersion and repulsion ( $\Delta G_{\text{vdw}}$ ), total internal energy ( $\Delta G_{\text{total}}$ ) and unbound system's energy ( $\Delta G_{\text{unb}}$ ) [105].

#### **2.4.2.Importance of Using Computational Simulation**

Molecular docking is primarily a computer simulation between a receptor and a ligand in order to predict interaction based on calculable variables and molecular properties.

A molecule's interaction orientation behaviors and conformational properties are essential when predicting its natural biological activity with a potentially active site. Specific attractiveness and repulsiveness are the basis of molecular recognition in biological practices. The primary purpose of computational simulation is to determine interactions between proteins and ligand via their 3D structural properties. Therefore molecular geometries and affinity properties of molecules are essential for interaction calculation. Also, it is crucial to be aware of the fact that molecular interactions function in an extremely non-additive way.

Fundamental biological processes like cell regulation, antibody-antigen identification, and enzyme inhibition, or signal transduction, transport, gene expression control, and multi-domain protein assembly incorporate important molecular interactions.

Experimental methods often costly and arduous when it comes to ascertaining stable protein-protein or protein-ligand complexes compared to computational molecular interaction calculation. Consequently, computational simulations are admittedly a fruitful solution for gaining knowledge about certain interactions [106-108].

Protein Data Bank (PDB) and the Worldwide Protein Data Bank (wwPDB) have almost a million protein structures. Such structures uploaded by many researchers

around the world created the opportunity for other researchers to tinker with those proteins to pave the way to other important investigations. Such as there are now binary complex structures databases available; in PDDBIND [109], PLD [110], AffinDB [111] and BindDB [112]. As time went by, because of the multiplying studies on proteins from before-mentioned resources, improvements are happening one after another [113].

### **2.4.3.Applications of Molecular Docking**

Molecular docking can be used as a tool for determination the feasibility of an experiment before doing the actual experiment. Hence there are some revolution-like findings where molecular docking is essential. In particular, ligand-protein interaction could possibly foretell the activation or inhibition of an enzyme. Rational drug designing could benefit from such results.

Protein purification is another field where molecular modeling could be of assistance. Determining the interaction among a target macromolecule and separation media provide ample information for efficient purification for the separation systems.

## **2.5.Software**

### **2.5.1.AutoDock and AutoGrid**

AutoDock is a molecular modeling simulation software primarily used for protein-ligand docking procedures for its effectiveness. The latest stable release is v.4.2.6, which was also the version used in this study. It is obtainable via download from its website. AutoDock is developed under GNU General Public License, and by the Scripps Research Institute [114].

AutoDockTools, or ADT for short, is the GUI component of AutoDock which makes it humanly possible to visualize the docking process as well as setting up rotatable bonds in the ligands and easing docking results analysis process.

AutoGrid is a grid calculation module for AutoDock. In the study, v4.2.6 was used

alongside AutoDock with AutoDockTools.

AutoDock helps researchers who study

- X-ray crystallography,
- structure-based drug design,
- lead optimization,
- virtual screening (HTS),
- combinatorial library design,
- protein-protein or protein-ligand docking,
- chemical mechanism research.

### **2.5.2.UCSF Chimera**

UCSF Chimera (or Chimera for short) is a highly extensible library-packed software package, which developed by the UCSF Resource for Biocomputing, Visualization, and Informatics, offers users to visualize interactive solutions and possibility to analyze data of molecular structures and other complementary information, such as density maps, supramolecular assemblies, sequence alignments, docking calculations, trajectories, and conformational ensembles to name a few [115, 116].

The latest stable release is v1.13.1, which was also the version used in this study.

### **2.5.3.Amber**

Amber is a software package that consists of a collection of countless sub-programs that work with each other to arrange, carry out, and examine molecular dynamics simulations. Amber helps the user with input files preparation. It also analyzes the gathered results in a comprehensive way. Amber named after molecular mechanics force fields, primarily modeled for the simulation of biomolecules [117].

#### **2.5.4. Antechamber**

Antechamber has a variety of additional modules for molecular mechanic (MM) studies. Antechamber is committed to solving the following problems while doing molecular mechanic calculations: (1) atom type identification; (2) bond type recognition; (2) evaluating the atomic equivalence; (3) residue topology file generation; (4) determining missing force field parameters and providing reasonable and similar substitutes. AmberTools has the Antechamber package as an accessory in its tools' gamut. With AmberTools, Antechamber can produce input automatically for most organic molecules in a database. Said algorithms doing these manipulations are possibly useful for other programs as well as Amber family of programs [118].

#### **2.5.5. MMTK**

MMTK which is an abbreviation of The Molecular Modeling Toolkit is an Open Source library. MMTK is used for molecular simulation applications whilst providing standard algorithms based turnkey implementations. While dealing with standard and non-standard issues in molecular simulations, MMTK can serve as a library for helping such situations, and it can be extended and modified [119].

### **2.6. Molecules**

#### **2.6.1. Human Serum Albumin (HSA)**

HSA is a vital healing proxy with high demand for the market. Proteins and drugs can be bound to HSA. Consequently, HSA is being monitored for an extensive selection of 64 triazine-based ligands at physiological conditions, being an inspirational figure, its binding and elution from human plasma conditions were neatly optimized [120].

Human plasma contains 30-50 g/l of HSA, which makes it the most available protein in it. HSA also has approximately 20 days of serum half-life [121] as well as osmotic pressure stabilization in veins whilst having a vital delivery job for fatty acids and hormones. Additionally, HSA can increase the circulation time of drug

pharmacokinetics, which is a drug carrier behavior. Meanwhile; hypovolemia, shock, trauma, and surgical blood loss used to be treated by HSA as a healing agent. HSA got its biopharmaceutical potential from being able to be found in different conditions such as a sole compound or a complex with other proteins [122]. The global plasma protein market has its 15% share in HSA, which is well over 20\$ Billion as of 2019 [123].

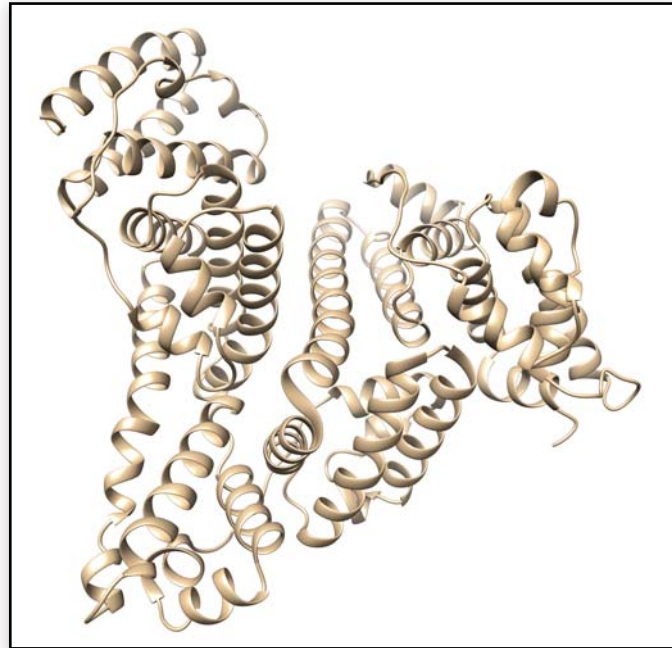


Figure 2.3. HSA ribbon structure

Presently, purification of HSA needs multiple unit operation acts, such as precipitation, heat-shock fractionation [124]. These processes also include ion-exchange chromatography and hydrophobic interaction chromatography as chromatographic methods [125,126].

Affinity chromatography still being used for protein purification regardless it has roots from the 1940s when Cohn first generate a blood surrogate for patients suffering from blood loss [127]. Therefore many affinity-based products are commercially available for the process now.

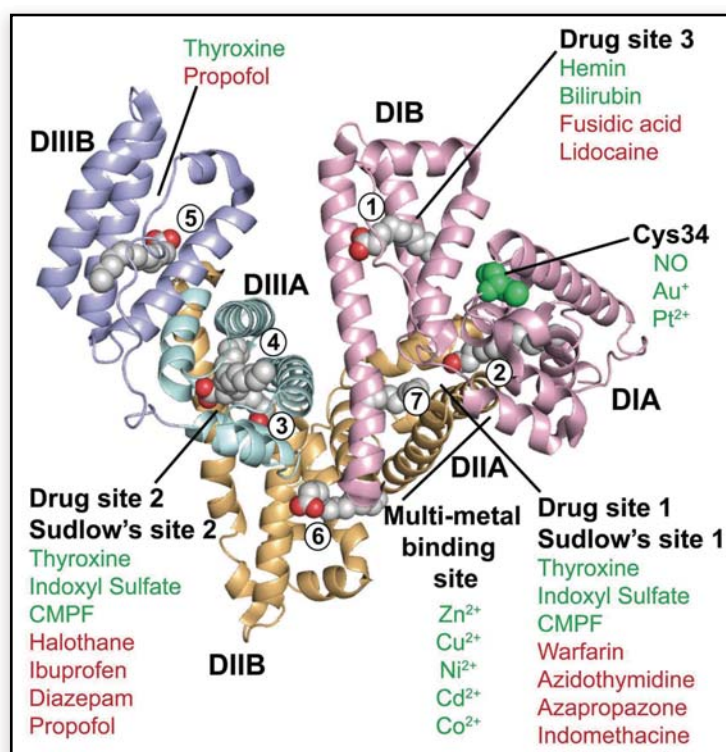


Figure 2.4. The crystal structure of HSA showing drug binding sites.

The clear structure of HSA solved in the saturated palmitic acid can be seen in Figure 2.4. The three domains (DI, DII, and DIII) consisted of  $\alpha$ -helical structures. Each domain and consecutively the structures are divided into subdomains (A and B) as indicated in the figure. The fatty acid binding site 1, the free cysteine (C34), and drug binding site 3 constitute the pink-colored domain of Domain I (DI). The other items in the figure colored green and red show endogenous and exogenous ligand binding sites, respectively [128].

### 2.6.2. Cibacron Blue (CBD)

Cibacron Blue F3GA is a relatively more obtainable substance for HSA purification, which was a sulfonated triazine dye-based adsorbent [129], in which low purity can be yielded by heterogeneous samples [130,131]. The use of triazine structuring drew attention at the end of the 1980s. It offers an advantageous strategy to develop low-priced, stable, and customized novel adsorbents for specific targets [132,133]. In particular, dissimilar ligands with triazine scaffold have been produced for a long time for immunoglobulins [134,135], insulin [136], and viral particles [137].

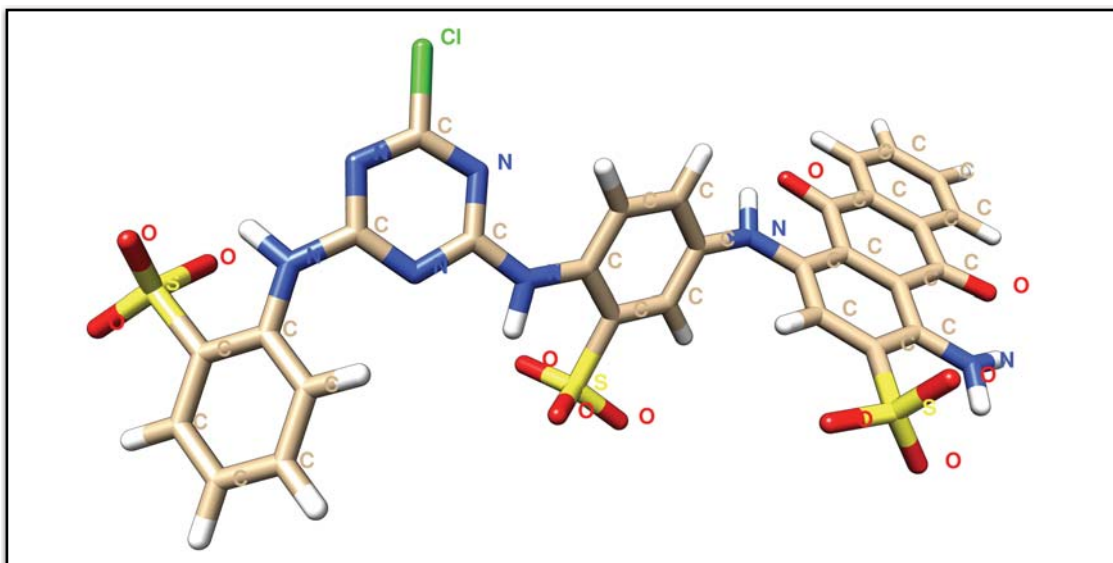


Figure 2.5. Cibacron Blue structure showing elements.





## **3.EXPERIMENT**

### **3.1.Hardware and Operating Systems**

The study was conveyed on an Apple iMac (Retina 5K, 27-inch, Late 2015, model identifier iMac17,1) with 4 GHz Intel Core i7 processor with 64-bit Skylake architecture which has Hyper-Threading enabled 4 cores with 8 threads, 32 GB 1867 MHz DDR3 RAM, 512GB SSD hard drive, and as GPU it has AMD Radeon R9 M395 with 2 GB VRAM. Operating system for the iMac is macOS Mojave (v10.14) which used as the primary system for biocomputing software UCSF Chimera, but for molecular modeling simulation software, AutoDock by the Scripps Research Institute was used on a virtual Microsoft Windows environment via hypervisor software VMWare Fusion v10 with a clean installation of Microsoft Windows 10 x64 (v1809) with 3 processing cores and 6144MB memory setting.

### **3.2.Softwares**

UCSF Chimera is a biocomputing software developed by the UCSF Resource for Biocomputing, Visualization, and Informatics (RBVI). In the study, v1.13.1 (build 41965) was used under macOS Mojave.

AutoDock is a molecular modeling simulation software developed by the Scripps Research Institute. In the study, v4.2.6 was used with the AutoDockTools GUI (Graphical User Interface) component v1.5.6.

AutoGrid is a grid calculation module for AutoDock developed by the Scripps Research Institute. In the study, v4.2.6 was used alongside AutoDock with AutoDockTools.

Amber is a software package that consists of a collection of numerous programs that work as a whole to arrange, carry out, and examine molecular dynamic simulations. Amber libraries were included in Chimera.

Antechamber has a variety of additional modules for molecular mechanic (MM)

studies. Antechamber algorithms were included in Chimera as well.

MMTK is an Open Source library for molecular simulation applications which provided minimization routines for UCSF Chimera.

### **3.3.Preparation of Macromolecules**

In the study;

- UCSF Chimera was used for minimization and dock preparation of ligand and protein structures.
- AutoGrid was used for pre-calculation of grids for the protein-ligand interaction.
- AutoDock was used for performing the docking process of the ligand to the grid of the target protein, in which grid was calculated by AutoGrid.
- AutoDockTools provided the GUI in order to ease the processing with AutoGrid and AutoDock.
- MMTK, the Molecular Modeling Toolkit, was used by Chimera for minimization routines.
- Amber and Amber's Antechamber module used for minimization processes.

#### **3.3.1.Structures from the PDB**

##### **3.3.1.1.Cibacron Blue (CBD)**

Structure of 1QRD, Cibacron Blue complexed with quinone reductase, FAD, and druoquinone, from the PDB was used as ligand structure source.

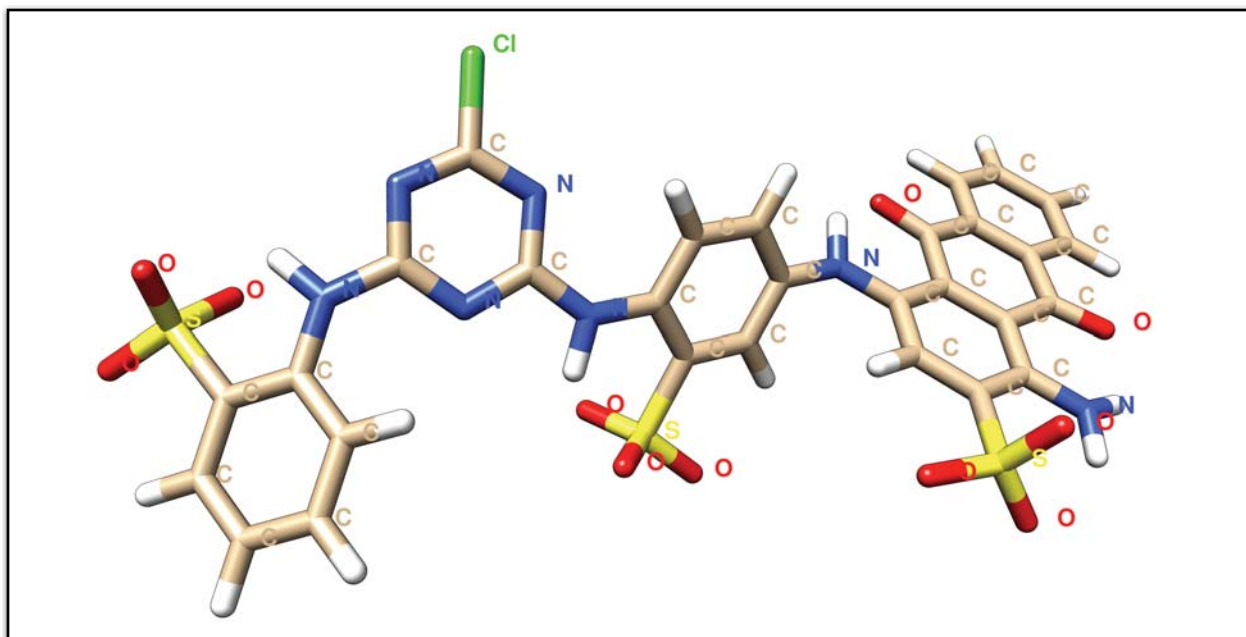


Figure 3.1. Cibacron Blue structure, minimized and prepared for docking.

Figure 3.1 shows the CBD structure generated from 1QRD, consequently minimized and prepared for docking [138].

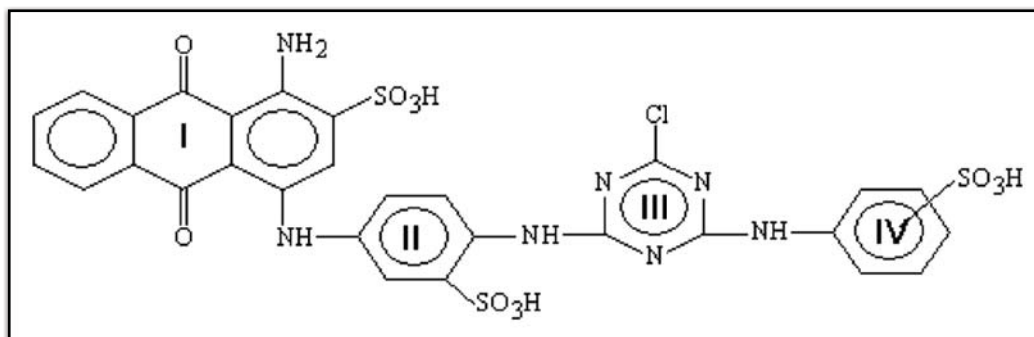


Figure 3.2. Cibacron Blue structure showing active regions [139].

In Figure 3.2, active regions shown as (I) anthraquinone and three (II, III, IV) diazine regions.

### 3.3.1.2. Human Serum Albumin (HSA)

The main structure for the HSA downloaded as a .pdb file inside UCSF Chimera from the Protein Data Bank (PDB) via entry of 2BXQ, which is human serum albumin complex containing myristate, phenylbutazone and indomethacin was

used as protein structure source.

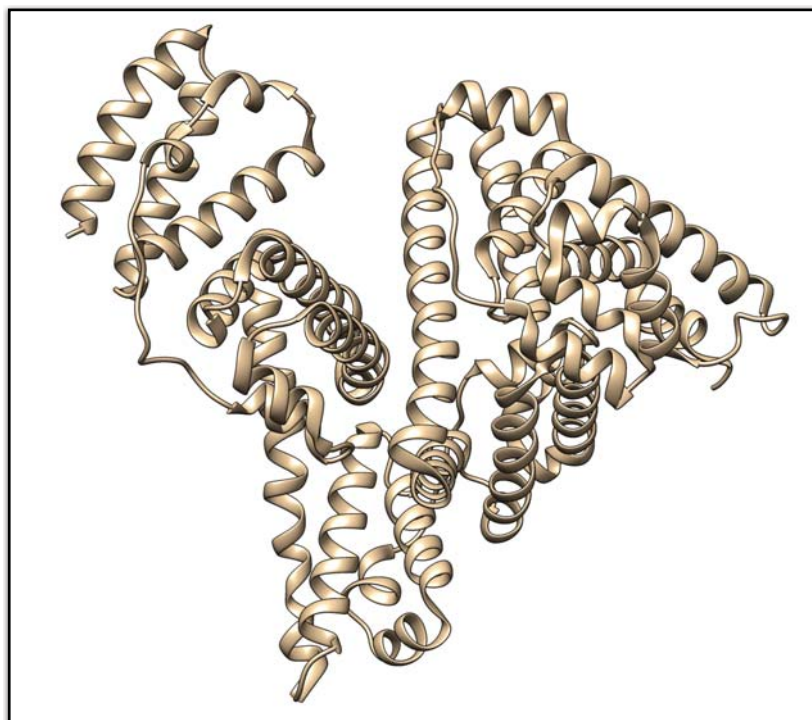


Figure 3.3. HSA structure, minimized, and prepared for docking.

Figure 3.3 shows the HSA structure generated from 2BXQ consequently minimized and prepared for docking [140].

### **3.4.Minimization and Dock Preparation**

UCSF Chimera software was used for minimization of structures then preparation for docking. Minimization command minimizes the energy of molecular models. In some cases minimization command optionally holds some atoms fixed. Minimization procedures are based on MMTK (Molecular Modeling Toolkit) algorithms, which is in UCSF Chimera's repository. For standard residues, Amber parameters and libraries were used. On the other hand, non-standard residues, Antechamber module provided parameters [141].

Prior to performing energy calculations, structural irregularities must be corrected. There is AddH command for adding hydrogens, and AddCharge command for assigning charges. Minimize command calls said commands before executing the Dock Prep command. As a result, prepared structures became available for

processing. While AddH and AddCharge commands are need-to-run basis, they were in fact ran in this study.

For the source of the protein structure, ProteinDataBank (PDB) was used via UCSF Chimera which means that UCSF Chimera downloaded the .pdb files itself hence there were no alterations possible on the file front. The downloaded file was started a new session in the software automatically. After removing the non-standard residues from the main structure, the minimization process was done with default parameters. H-bonds were also considered while adding hydrogens for Dock Prep. For incomplete side chains, Dunbrack 2010 rotamer library was used [142]. Then AMBER ff14SB was used for standard residue charge calculation. For other residues, Gasteiger from Amber's Antechamber module was used [143]. Gasteiger method is based on iterative partial equalization of orbital electronegativity also it is faster and more approximate than its counterpart.

#### **3.4.1.Targeting Binding Sites**

The target protein was preserved rigid throughout the docking process, while drug molecules were allowed flexibility. The search area was defined to cover two distinct HSA drug-binding sites. Binding Site 1 (BS1) was covered within a region with coordinates at the center along the X, Y and Z axis as -4.326, -4.756 and 9.449 respectively, and dimensions (Å) along the X, Y and Z axis were set to 10 Å. In Binding Site 2, the search area region was centered at the coordinates (X, Y, Z) 9.187, 3.021, -14.306 respectively while the dimensions along these axes were also set to 10 Å [144].

For conformations 1 to 4, a cubical lattice of  $126 \times 126 \times 126$  points was used in which the values show each point count through x, y, and z coordinates with a spacing of 0.375 Å. Docking simulations were conducted with 150 as population size and  $1.0 \times 10^7$  number of evaluations [145] using Lamarckian Genetic Algorithm v4.2.

For conformations 5 and 6, a cubical lattice of  $60 \times 60 \times 60$  points was used in which the values show each point count through x, y, and z coordinates with a spacing of 0.375 Å. Docking simulations were conducted with 150 as population

size and  $2.5 \times 10^6$  number of evaluations using Lamarckian Genetic Algorithm v4.2.

All conformations had a 10 run of GA with 150 as population size and a 27000 maximum number of generations. Other values were left as is.

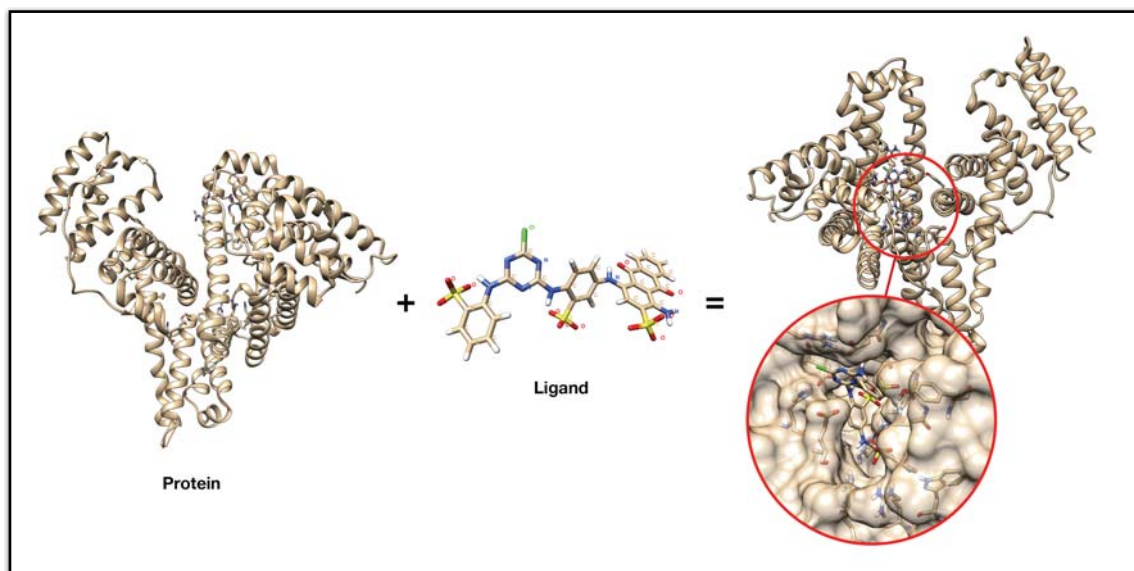


Figure 3.4. Docking of CBD on HSA.

Figure 3.4 shows visual representation of docking of CBD to HSA.

## **4.RESULT AND DISCUSSION**

AutoDock v4.2.6 was used for docking CBD to identify active locations for specific targeting of binding sites on HSA. For trials, Lamarckian Genetic Algorithm (LGA) was used with several different configurations such as evaluation counts of  $2.5 \times 10^6$  and  $1.0 \times 10^7$ . Grid box sizes differ as  $60 \times 60 \times 60$  and  $126 \times 126 \times 126$  for different conformation simulations as well as target coordinates change from default to BS1 to BS2 which all will be explicitly mentioned for each conformation.

### **4.1.Results**

#### **4.1.1.Conformation 1**

For conformation 1, a grid box of  $126 \times 126 \times 126$  was used with  $1.0 \times 10^7$  evaluations, and Binding Site 1 was targeted.

##### **4.1.1.1.Cluster Analysis for Conformation 1**

Conformation 1 was the lowest energy ranked of 10 conformations in this analysis. The RMSD cluster analyses were performed using 56 of 56 total atoms and using ligand atoms only.

Structurally similar clusters were shown in Table 4.1 sorted by increasing energy.

Distinct conformational clusters count in total of 10 runs was 10 while using an RMSD tolerance of 2.0 Å. Moreover, docking analyses were performed at 298.15 K temperature.

##### **4.1.1.1.1.Clustering Histogram Data for Conformation 1**

Data was collected while performing docking one molecule of CBD to HSA on BS1.

Table 4.1. Clustering Histogram data for Conformation 1

| Clustering Rank | LBE (Kcal/mol) | Run Count | MBE (Kcal/mol) |
|-----------------|----------------|-----------|----------------|
| 1               | -9.23          | 1         | -9.23          |
| 2               | -8.89          | 3         | -8.89          |
| 3               | -8.52          | 7         | -8.52          |
| 4               | -8.14          | 9         | -8.14          |
| 5               | -7.94          | 2         | -7.94          |
| 6               | -7.37          | 10        | -7.37          |
| 7               | -7.19          | 5         | -7.19          |
| 8               | -6.65          | 4         | -6.65          |
| 9               | -6.55          | 8         | -6.55          |
| 10              | -5.94          | 6         | -5.94          |

All ranks had a Number in Cluster value of 1.

#### 4.1.1.1.2.RMSD Table for Conformation 1

Table 4.2. RMSD Values and Binding Energies of each run on Conformation 1.

| Rank | Run Order | Binding Energy(Kcal/mol) | Reference RMSD |
|------|-----------|--------------------------|----------------|
| 1    | 1         | -9.23                    | 36.44          |
| 2    | 3         | -8.89                    | 34.70          |
| 3    | 7         | -8.52                    | 32.79          |
| 4    | 9         | -8.14                    | 26.82          |
| 5    | 2         | -7.94                    | 27.08          |
| 6    | 10        | -7.37                    | 37.68          |
| 7    | 5         | -7.19                    | 32.59          |
| 8    | 4         | -6.65                    | 35.94          |
| 9    | 8         | -6.55                    | 32.84          |
| 10   | 6         | -5.94                    | 29.11          |

All ranks had a Sub-Rank value of 1 and Cluster RMSD value of 0.00.



#### 4.1.1.2. Information Entropy for Cluster 1 of Conformation 1

Information entropy for cluster rank 1 of conformation 1 is 1.00 with a root mean square tolerance for reclustering of 2.00 Å.

#### 4.1.1.3. Thermodynamic Analysis for Conformation 1

Partition function for Conf 1,  $Q = 10.13$   
Free energy for Conf 1,  $G \sim -1371.88$  (kcal/mol)  
Internal energy for Conf 1,  $U = -7.64$  (kcal/mol)

All results were for 298.15 K temperature and entropy (S) was 4.58 kcal/mol/K.

#### 4.1.1.4. Lowest Ranked Docking of Conformation 1

Table 4.3. Data for Lowest Energy Docking of Conformation 1

|                                      |                       |
|--------------------------------------|-----------------------|
| Run order                            | 1                     |
| Rank of cluster                      | 1                     |
| Conformation count in this cluster   | 1                     |
| Reference structure RMSD value       | 36.445 Å              |
| <b>Evaluated Binding Free Energy</b> | <b>-9.23 kcal/mol</b> |
| Evaluated Inhibition Constant, Ki    | 172.03 nM (nanomolar) |
| Final Intermolecular Energy          | -12.21 kcal/mol       |
| vdW + Hbond + desolv Energy          | -7.59 kcal/mol        |
| Electrostatic Energy                 | -4.62 kcal/mol        |
| Final Total Internal Energy          | -5.87 kcal/mol        |

Torsional free energy is +2.98 kcal/mol and unbound system's energy is the same as the final total internal energy.

## 4.1.2. Conformation 2

For conformation 2, a grid box of  $126 \times 126 \times 126$  was used with  $1.0 \times 10^7$  evaluations, and Binding Site 2 was targeted.

### 4.1.2.1. Cluster Analysis for Conformation 2

Conformation 2 was the lowest energy ranked of 10 conformations in this analysis. The RMSD cluster analyses were performed using 56 of 56 total atoms and using ligand atoms only.

Structurally similar clusters were shown in Table 4.4 sorted by increasing energy.

Distinct conformational clusters count in a total of 10 runs was 10 while using an RMSD tolerance of 2.0 Å. Moreover, docking analyses were performed at 298.15 K temperature.

#### 4.1.2.1.1. Clustering Histogram Data for Conformation 2

Data was collected while performing docking one molecule of CBD to HSA.

Table 4.4. Clustering Histogram data for Conformation 2

| Clustering Rank | LBE (Kcal/mol) | Run Count | MBE (Kcal/mol) |
|-----------------|----------------|-----------|----------------|
| 1               | -6.08          | 5         | -6.08          |
| 2               | -5.89          | 4         | -5.89          |
| 3               | -5.72          | 8         | -5.72          |
| 4               | -5.60          | 2         | -5.60          |
| 5               | -5.55          | 9         | -5.55          |
| 6               | -5.33          | 3         | -5.33          |
| 7               | -5.09          | 1         | -5.09          |
| 8               | -5.06          | 7         | -5.06          |
| 9               | -4.83          | 6         | -4.83          |
| 10              | -3.54          | 10        | -3.54          |

All ranks had a Number in Cluster value of 1.

#### 4.1.2.1.2.RMSD Table for Conformation 2

Table 4.5. RMSD Values and Binding Energies of each run on Conformation 2.

| Rank | Run Order | Binding Energy(Kcal/mol) | Reference RMSD |
|------|-----------|--------------------------|----------------|
| 1    | 5         | -6.08                    | 41.12          |
| 2    | 4         | -5.89                    | 43.91          |
| 3    | 8         | -5.72                    | 38.27          |
| 4    | 2         | -5.60                    | 46.31          |
| 5    | 9         | -5.55                    | 27.17          |
| 6    | 3         | -5.33                    | 41.65          |
| 7    | 1         | -5.09                    | 41.18          |
| 8    | 7         | -5.06                    | 22.26          |
| 9    | 6         | -4.83                    | 30.39          |
| 10   | 10        | -3.54                    | 43.47          |

All ranks had a Sub-Rank value of 1 and Cluster RMSD value of 0.00.

#### 4.1.2.2. Information Entropy for Cluster 1 of Conformation 2

Information entropy for cluster 1 of conformation 2 is 1.00 with a root mean square tolerance for reclustering of 2.00 Å.

#### 4.1.2.3. Thermodynamic Analysis for Conformation 2

Partition function for Conf 2,  $Q = 10.09$

Free energy for Conf 2,  $G \sim -1369.51$  (kcal/mol)

Internal energy for Conf 2,  $U = -5.27$  (kcal/mol)

All results were for 298.15 K temperature and entropy (S) was 4.58 kcal/mol/K.

#### 4.1.2.4.Lowest Ranked Docking of Conformation 2

Table 4.6. Data for Lowest Energy Docking of Conformation 2

|                                      |                       |
|--------------------------------------|-----------------------|
| Run order                            | 5                     |
| Rank of cluster                      | 1                     |
| Conformation count in this cluster   | 1                     |
| Reference structure RMSD value       | 41.116 Å              |
| <b>Evaluated Binding Free Energy</b> | <b>-6.08 kcal/mol</b> |
| Estimated Inhibition Constant, Ki    | 34.67 µM (micromolar) |
| Final Intermolecular Energy          | -9.07 kcal/mol        |
| vdW + Hbond + desolv Energy          | -8.05 kcal/mol        |
| Electrostatic Energy                 | -1.01 kcal/mol        |
| Final Total Internal Energy          | -5.62 kcal/mol        |

Torsional free energy is +2.98 kcal/mol and unbound system's energy is the same as the final total internal energy.

#### 4.1.3.Conformation 3

For conformation 3, a grid box of 126 × 126 × 126 was used with 1.0 × 10<sup>7</sup> evaluations, and Binding Site 1 was targeted.

##### 4.1.3.1.Cluster Analysis for Conformation 3

Conformation 3 was the lowest energy ranked of 10 conformations in this analysis. The RMSD cluster analyses were performed using 56 of 56 total atoms and using ligand atoms only.

Structurally similar clusters were shown in Table 4.7 sorted by increasing energy.

Distinct conformational clusters count in a total of 10 runs was 10 while using an RMSD tolerance of 2.0 Å. Moreover, docking analyses were performed at 298.15 K temperature.

#### 4.1.3.1.1. Clustering Histogram Data for Conformation 3

Data was collected while performing docking one molecule of CBD to HSA.

Table 4.7. Clustering Histogram data for Conformation 3

| Clustering Rank | LBE (Kcal/mol) | Run Count | MBE (Kcal/mol) |
|-----------------|----------------|-----------|----------------|
| 1               | -12.64         | 7         | -12.64         |
| 2               | -12.31         | 10        | -12.31         |
| 3               | -11.41         | 5         | -11.41         |
| 4               | -11.39         | 9         | -11.39         |
| 5               | -10.98         | 2         | -10.98         |
| 6               | -10.74         | 8         | -10.74         |
| 7               | -10.04         | 6         | -10.04         |
| 8               | -9.91          | 4         | -9.91          |
| 9               | -9.86          | 1         | -9.86          |
| 10              | -8.71          | 3         | -8.71          |

All ranks had a Number in Cluster value of 1.

#### 4.1.3.1.2. RMSD Table for Conformation 3

Table 4.8. RMSD Values and Binding Energies of each run on Conformation 3.

| Rank | Run Order | Binding Energy(Kcal/mol) | Reference RMSD |
|------|-----------|--------------------------|----------------|
| 1    | 7         | -12.64                   | 11.67          |
| 2    | 10        | -12.31                   | 11.75          |
| 3    | 5         | -11.41                   | 12.52          |
| 4    | 9         | -11.39                   | 12.46          |
| 5    | 2         | -10.98                   | 12.53          |
| 6    | 8         | -10.74                   | 10.66          |
| 7    | 6         | -10.04                   | 12.81          |
| 8    | 4         | -9.91                    | 11.89          |
| 9    | 1         | -9.86                    | 12.69          |
| 10   | 3         | -8.71                    | 10.39          |

All ranks had a Sub-Rank value of 1 and Cluster RMSD value of 0.00.

#### 4.1.3.2. Information Entropy for Cluster 1 of Conformation 3

Information entropy for cluster 1 of conformation 3 is 1.00 with a root mean square tolerance for reclustering of 2.00 Å.

#### 4.1.3.3. Thermodynamic Analysis for Conformation 3

Partition function for Conf 3,  $Q = 10.18$   
Free energy for Conf 3,  $G \sim -1375.04$  kcal/mol  
Internal energy for Conf 3,  $U = -10.80$  kcal/mol

All results were for 298.15 K temperature and entropy (S) was 4.58 kcal/mol/K.

#### 4.1.3.4. Lowest Ranked Docking of Conformation 3

Table 4.9. Data for Lowest Energy Docking of Conformation 3

|                                      |                        |
|--------------------------------------|------------------------|
| Run order                            | 7                      |
| Rank of cluster                      | 1                      |
| Conformation count in this cluster   | 1                      |
| Reference structure RMSD value       | 11.672 Å               |
| <b>Evaluated Binding Free Energy</b> | <b>-12.64 kcal/mol</b> |
| Evaluated Inhibition Constant, $K_i$ | 544.23 pM (picomolar)  |
| Final Intermolecular Energy          | -15.62 kcal/mol        |
| vdW + Hbond + desolv Energy          | -14.38 kcal/mol        |
| Electrostatic Energy                 | -1.24 kcal/mol         |
| Final Total Internal Energy          | -6.44 kcal/mol         |

Torsional free energy is +2.98 kcal/mol and unbound system's energy is the same as the final total internal energy.

#### 4.1.4. Conformation 4

For conformation 4, a grid box of  $126 \times 126 \times 126$  was used with  $1.0 \times 10^7$  evaluations, and Binding Site 2 was targeted.

##### 4.1.4.1. Cluster Analysis for Conformation 4

Conformation 4 was the lowest energy ranked of 10 conformations in this analysis. The RMSD cluster analyses were performed using 56 of 56 total atoms and using ligand atoms only.

Structurally similar clusters were shown in Table 4.10 sorted by increasing energy.

Distinct conformational clusters count in a total of 10 runs was 10 while using an RMSD tolerance of 2.0 Å. Moreover, docking analyses were performed at 298.15 K temperature.

##### 4.1.4.1.1. Clustering Histogram Data for Conformation 4

Data was collected while performing docking one molecule of CBD to HSA.

Table 4.10. Clustering Histogram data for Conformation 4.

| Clustering Rank | LBE (Kcal/mol) | Run Count | MBE (Kcal/mol) |
|-----------------|----------------|-----------|----------------|
| 1               | -13.75         | 5         | -13.75         |
| 2               | -12.46         | 9         | -12.46         |
| 3               | -11.63         | 4         | -11.63         |
| 4               | -11.37         | 6         | -11.37         |
| 5               | -10.89         | 8         | -10.89         |
| 6               | -10.32         | 3         | -10.32         |
| 7               | -9.82          | 2         | -9.82          |
| 8               | -9.66          | 7         | -9.66          |
| 9               | -9.18          | 10        | -9.18          |
| 10              | -8.79          | 1         | -8.79          |

All ranks had a Number in Cluster value of 1.

#### 4.1.4.1.2.RMSD Table for Conformation 4

Table 4.11. RMSD Values and Binding Energies of each run on Conformation 4.

| Rank | Run Order | Binding Energy(Kcal/mol) | Reference RMSD |
|------|-----------|--------------------------|----------------|
| 1    | 5         | -13.75                   | 13.20          |
| 2    | 9         | -12.46                   | 12.00          |
| 3    | 4         | -11.63                   | 11.50          |
| 4    | 6         | -11.37                   | 6.96           |
| 5    | 8         | -10.89                   | 11.33          |
| 6    | 3         | -10.32                   | 11.17          |
| 7    | 2         | -9.82                    | 11.25          |
| 8    | 7         | -9.66                    | 11.76          |
| 9    | 10        | -9.18                    | 10.82          |
| 10   | 1         | -8.79                    | 12.74          |

All ranks had a Sub-Rank value of 1 and Cluster RMSD value of 0.00.

#### 4.1.4.2. Information Entropy for Cluster 1 of Conformation 4

Information entropy for cluster 1 of conformation 4 is 1.00 with a root mean square tolerance for reclustering of 2.00 Å.

#### 4.1.4.3. Thermodynamic Analysis for Conformation 4

Partition function for Conf 4,  $Q = 10.18$

Free energy for Conf 4,  $G \sim -1375.03$  (kcal/mol)

Internal energy for Conf 4,  $U = -10.79$  (kcal/mol)

All results were for 298.15 K temperature and entropy (S) was 4.58 kcal/mol/K.



#### 4.1.4.4.Lowest Ranked Docking of Conformation 4

Table 4.12. Data for Lowest Energy Docking of Conformation 4

|                                      |                        |
|--------------------------------------|------------------------|
| Run order                            | 5                      |
| Rank of cluster                      | 1                      |
| Conformation count in this cluster   | 1                      |
| Reference structure RMSD value       | 13.202 Å               |
| <b>Evaluated Binding Free Energy</b> | <b>-13.75 kcal/mol</b> |
| Evaluated Inhibition Constant, Ki    | 84.08 pM (picomolar)   |
| Final Intermolecular Energy          | -16.73 kcal/mol        |
| vdW + Hbond + desolv Energy          | -15.21 kcal/mol        |
| Electrostatic Energy                 | -1.51 kcal/mol         |
| Final Total Internal Energy          | -6.51 kcal/mol         |

Torsional free energy is +2.98 kcal/mol and unbound system's energy is the same as the final total internal energy.

#### 4.1.5.Conformation 5

For conformation 5, a grid box of 60 × 60 × 60 was used with 2.5 × 10<sup>6</sup> evaluations and default grid coordinates were used, hence no binding site was specifically targeted.

##### 4.1.5.1.Cluster Analysis for Conformation 5

Conformation 5 was the lowest energy ranked of 10 conformations in this analysis. The RMSD cluster analyses were performed using 56 of 56 total atoms and using ligand atoms only.

Structurally similar clusters were shown in Table 4.13 sorted by increasing energy.

Distinct conformational clusters count in a total of 10 runs was 10 while using an RMSD tolerance of 2.0 Å. Moreover, docking analyses were performed at 298.15 K temperature.

#### 4.1.5.1.1.Clustering Histogram Data for Conformation 5

Data was collected while performing docking one molecule of CBD to HSA

Table 4.13. Clustering Histogram data for Conformation 5.

| Clustering Rank | LBE (Kcal/mol) | Run Count | MBE (Kcal/mol) |
|-----------------|----------------|-----------|----------------|
| 1               | -13.69         | 1         | -13.69         |
| 2               | -12.40         | 3         | -12.40         |
| 3               | -9.94          | 4         | -9.94          |
| 4               | -9.28          | 2         | -9.28          |
| 5               | -8.71          | 6         | -8.71          |
| 6               | -8.49          | 10        | -8.49          |
| 7               | -8.36          | 7         | -8.36          |
| 8               | -8.18          | 8         | -8.18          |
| 9               | -7.53          | 5         | -7.53          |
| 10              | -6.57          | 9         | -6.57          |

All ranks had a Number in Cluster value of 1.

#### 4.1.5.1.2.RMSD Table for Conformation 5

Table 4.14. RMSD Values and Binding Energies of each run on Conformation 5.

| Rank | Run Order | Binding Energy(Kcal/mol) | Reference RMSD |
|------|-----------|--------------------------|----------------|
| 1    | 1         | -13.69                   | 10.88          |
| 2    | 3         | -12.40                   | 11.30          |
| 3    | 4         | -9.94                    | 10.83          |
| 4    | 2         | -9.28                    | 10.53          |
| 5    | 6         | -8.71                    | 9.43           |
| 6    | 10        | -8.49                    | 11.63          |
| 7    | 7         | -8.36                    | 9.92           |
| 8    | 8         | -8.18                    | 10.28          |
| 9    | 5         | -7.53                    | 8.97           |
| 10   | 9         | -6.57                    | 8.70           |

All ranks had a Sub-Rank value of 1 and Cluster RMSD value of 0.00.

#### 4.1.5.2. Information Entropy for Cluster 1 of Conformation 5

Information entropy for cluster 1 of conformation 5 is 1.00 with a root mean square tolerance for reclustering of 2.00 Å.

#### 4.1.5.3. Thermodynamic Analysis for Conformation 5

Partition function for Conf 5,  $Q = 10.16$   
Free energy for Conf 5,  $G \sim -1373.56$  (kcal/mol)  
Internal energy for Conf 5,  $U = -9.32$  (kcal/mol)

All results were for 298.15 K temperature and entropy (S) was 4.58 kcal/mol/K.

#### 4.1.5.4. Lowest Ranked Docking of Conformation 5

Table 4.15. Data for Lowest Energy Docking of Conformation 5

|   |                      |
|---|----------------------|
| Run order                                       | 1                    |
| Rank of cluster                                 | 1                    |
| Conformation count in this cluster              | 1                    |
| Reference structure RMSD value                  | 10.884 Å             |
| <b>Evaluated Binding Free Energy (kcal/mol)</b> | <b>-13.69</b>        |
| Evaluated Inhibition Constant, $K_i$            | 91.58 pM (picomolar) |
| Final Intermolecular Energy (kcal/mol)          | -16.68               |
| vdW + Hbond + desolv Energy (kcal/mol)          | -11.91               |
| Electrostatic Energy (kcal/mol)                 | -4.77                |
| Final Total Internal Energy (kcal/mol)          | -5.92                |

Torsional free energy is +2.98 kcal/mol and unbound system's energy is the same as the final total internal energy.

#### 4.1.6. Conformation 6

For conformation 6, a grid box of  $60 \times 60 \times 60$  was used with  $2.5 \times 10^6$  evaluations

and default grid coordinates were used, hence no binding site was specifically targeted.

#### 4.1.6.1. Cluster Analysis for Conformation 6

Conformation 6 was the lowest energy ranked of 10 conformations in this analysis. The RMSD cluster analyses were performed using 56 of 56 total atoms and using ligand atoms only.

Structurally similar clusters were shown in Table 4.16 sorted by increasing energy.

Distinct conformational clusters count in a total of 10 runs was 8 while using an RMSD tolerance of 2.0 Å. Moreover, docking analyses were performed at 298.15 K temperature.

##### 4.1.6.1.1. Clustering Histogram Data for Conformation 6

Data was collected while performing docking one molecule of CBD to HSA.

Table 4.16. Clustering Histogram data for Conformation 6.

| Clustering Rank | LBE (Kcal/mol) | Run Count | MBE (Kcal/mol) | Number in Cluster |
|-----------------|----------------|-----------|----------------|-------------------|
| 1               | -10.73         | 4         | -10.73         | 1                 |
| 2               | -10.71         | 7         | -9.65          | 3                 |
| 3               | -10.38         | 2         | -10.38         | 1                 |
| 4               | -9.78          | 10        | -9.78          | 1                 |
| 5               | -9.69          | 1         | -9.69          | 1                 |
| 6               | -8.08          | 5         | -8.08          | 1                 |
| 7               | -7.79          | 3         | -7.79          | 1                 |
| 8               | -7.18          | 8         | -7.18          | 1                 |

#### 4.1.6.1.2.RMSD Table for Conformation 6

Table 4.17. RMSD Values and Binding Energies of each run on Conformation 6.

| Rank | Sub-Rank | Run Order | Binding Energy(Kcal/mol) | Cluster RMSD | Reference RMSD |
|------|----------|-----------|--------------------------|--------------|----------------|
| 1    | 1        | 4         | -10.73                   | 0.00         | 8.65           |
| 2    | 1        | 7         | -10.71                   | 0.00         | 8.41           |
| 2    | 2        | 9         | -10.09                   | 1.70         | 9.24           |
| 2    | 3        | 6         | -8.14                    | 1.48         | 8.66           |
| 3    | 1        | 2         | -10.38                   | 0.00         | 9.02           |
| 4    | 1        | 10        | -9.78                    | 0.00         | 11.22          |
| 5    | 1        | 1         | -9.69                    | 0.00         | 9.71           |
| 6    | 1        | 5         | -8.08                    | 0.00         | 9.46           |
| 7    | 1        | 3         | -7.79                    | 0.00         | 7.86           |
| 8    | 1        | 8         | -7.18                    | 0.00         | 7.91           |

#### 4.1.6.2.Information Entropy for Cluster 1 of Conformation 6

Information entropy for cluster 1 of conformation 6 is 0.86 with a root mean square tolerance for reclustering of 2.00 Å.

#### 4.1.6.3. Thermodynamic Analysis for Conformation 6

Partition function for Conf 6,  $Q = 10.16$

Free energy for Conf 6,  $G \sim -1373.50$  (kcal/mol)

Internal energy for Conf 6,  $U = -9.26$  (kcal/mol)

All results were for 298.15 K temperature and entropy (S) was 4.58 kcal/mol/K.

#### 4.1.6.4.Lowest Ranked Docking of Conformation 6

Table 4.18. Data for Lowest Energy Docking of Conformation 6

|   |                      |
|---|----------------------|
| Run order                                       | 4                    |
| Rank of cluster                                 | 1                    |
| Conformation count in this cluster              | 1                    |
| Reference structure RMSD value                  | 8.653 A              |
| <b>Evaluated Binding Free Energy (kcal/mol)</b> | <b>-10.73</b>        |
| Evaluated Inhibition Constant, Ki               | 13.74 nM (nanomolar) |
| Final Intermolecular Energy (kcal/mol)          | -13.71               |
| vdW + Hbond + desolv Energy (kcal/mol)          | -9.13                |
| Electrostatic Energy (kcal/mol)                 | -4.58                |
| Final Total Internal Energy (kcal/mol)          | -4.75                |

Torsional free energy is +2.98 kcal/mol and unbound system's energy is the same as the final total internal energy.

## 4.2.DISCUSSION

### 4.2.1.Binding Affinity of CBD to Human Serum Albumin (HSA)

Six conformations of CBD were implemented in AutoDock v6.2 software for predicting the binding preference of CBD to HSA. Conformation, grid and grid box features, and binding site, free energy and possibility of CBD interaction with HSA were listed in Table 4.19.

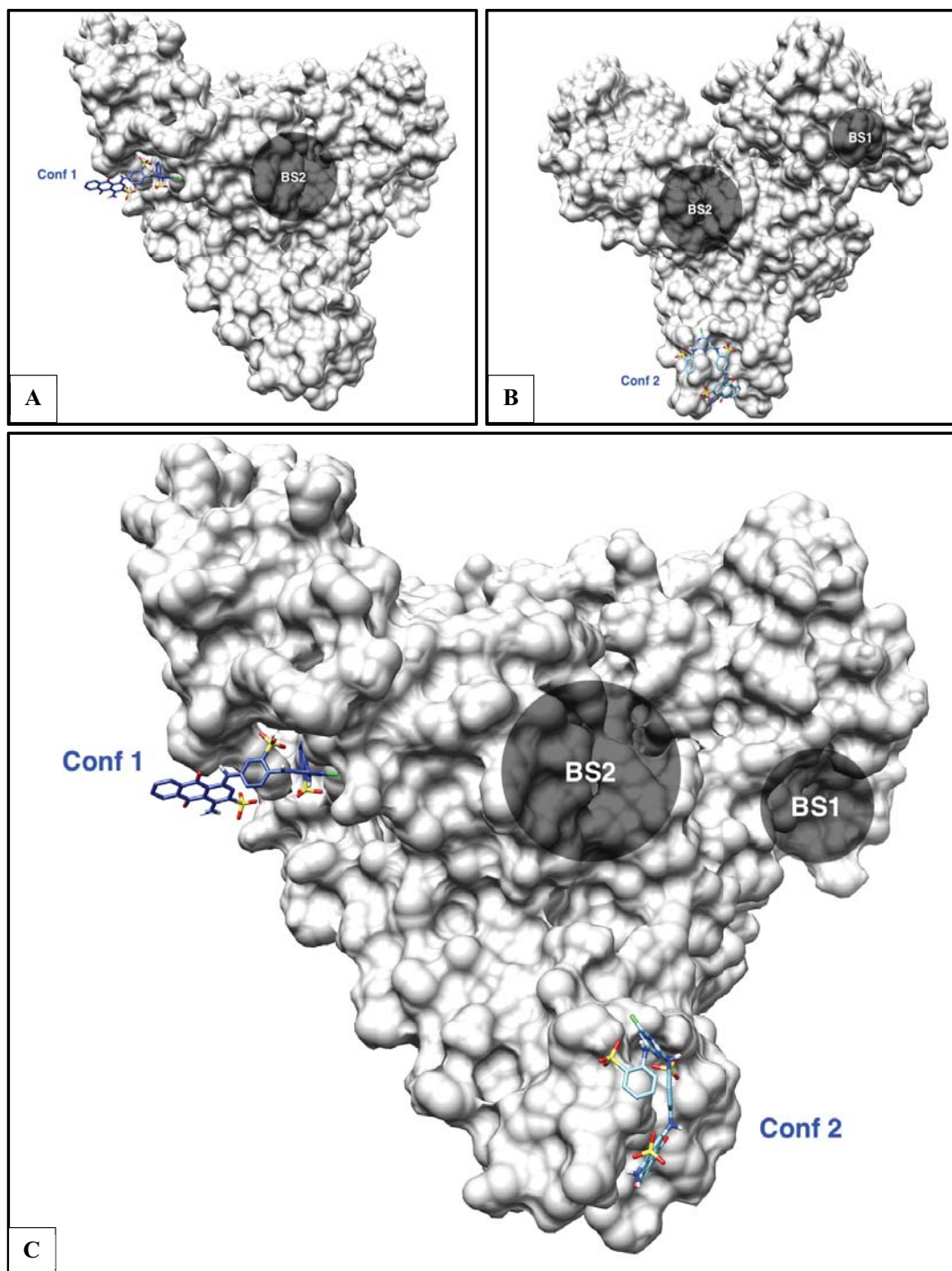
Table 4.19. Conformation features and binding free energies of CBD bound to HSA.

| Conformation # | Grid box        | Grid           | Evaluation                | Binding Site | Binding Energy (kcal/mol) | Binding Possibility |
|----------------|-----------------|----------------|---------------------------|--------------|---------------------------|---------------------|
| 1              | 126/126/126     | BS1            | 1.0x10 <sup>7</sup>       | Default      | -9.12                     | No Binding          |
| 2              | 126/126/126     | BS2            | 1.0x10 <sup>7</sup>       | Default      | -6.08                     | No Binding          |
| 3              | 126/126/126     | BS1            | 1.0x10 <sup>7</sup>       | BS3          | -12.64                    | Favorable           |
| 4              | 126/126/126     | BS2            | 1.0x10 <sup>7</sup>       | BS1          | -13.75                    | No Binding          |
| <b>5</b>       | <b>60/60/60</b> | <b>Default</b> | <b>2.5x10<sup>6</sup></b> | <b>BS2</b>   | <b>-13.69</b>             | <b>Favorable</b>    |
| 6              | 60/60/60        | Default        | 2.5x10 <sup>6</sup>       | BS1          | -10.74                    | Favorable           |

In the process, only DockPrep command was used for dock preparation for Conf #3, 4, and 5. Although for Conf #1, 2, and 4 Min command was used alongside DockPrep as well. Also, all conformations were implemented by Gasteiger Method in the AutoDock software.

According to Table 4.19; Although the binding free energy of Conf # 1, 2 and 4 are favorable as -9.12, -6.08 and -12.64, respectively, they indicate no binding possibility since CBD is located out of binding sites. The reason why is explained in sections 4.2.2 and 4.2.3 in detail. Conf # 3, 5, and 6 have favorable binding energy. Among these, Conf # 5 (in bold) has the most favorable binding free

energy as -13.69 kcal/mol, which is located to binding site 2 of HSA.



#### 4.2.2. Binding Properties of CBD docked to HSA for Conf #1 and Conf #2

Figure 4.1. A) Conformation 1, B) Conformation 2, C) Conformation 1 and 2 of CBD interaction with HSA (solid grey surface).



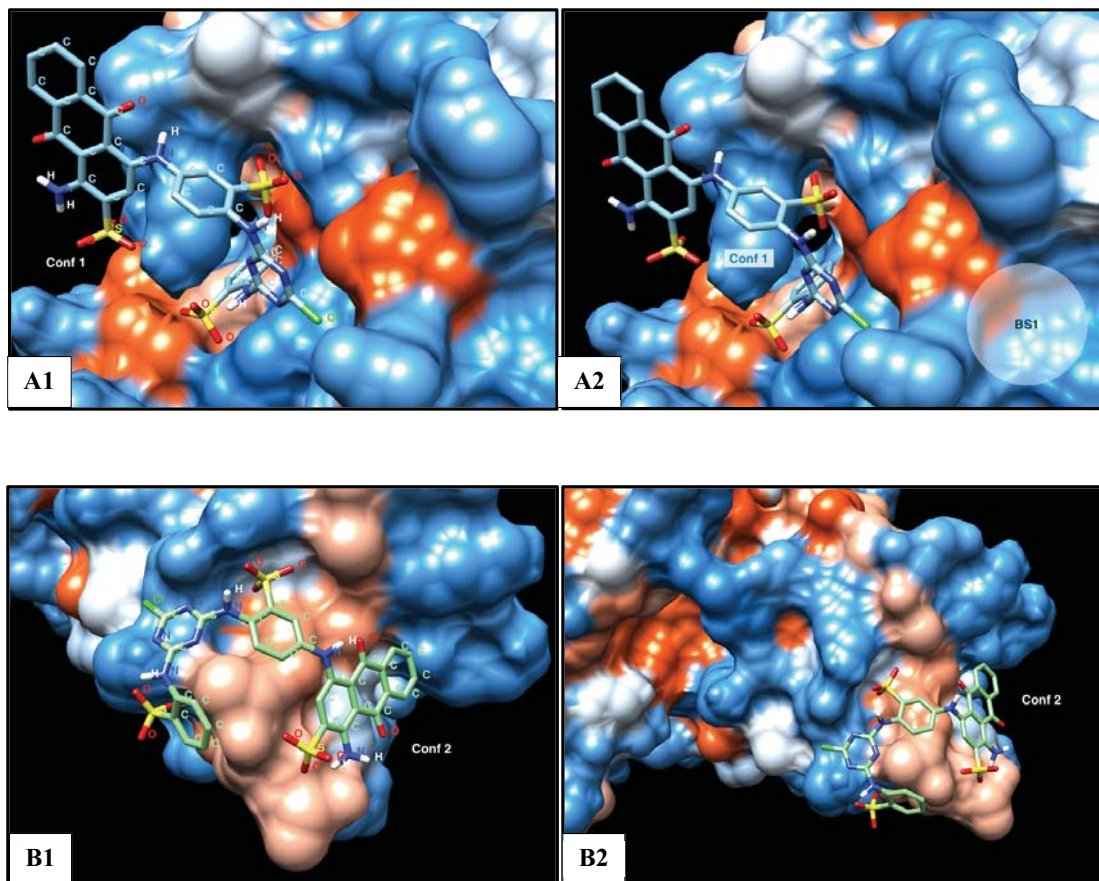


Figure 4.2. A) Conformation 1 and B) Conformation 2 of CBD interaction with HSA interactive hydrophobicity solid surface. (Dodger blue denotes more hydrophilic surface and orange denotes more hydrophobic surface.)

As seen in Figure 4.2, Conf #1 and #2 of CBD interacts with HSA. Note that; the surface of HSA is interactive hydrophobicity solid surface. This view has the coloring of "hydrophobicity surface" preset in which color scales for most hydrophilic areas as dodger blue, and the most hydrophobic areas as orange-red with white in between. The CBD-binding pocket is blue and orange, pointing out its both hydrophilic and hydrophobic character. However, Conformations #1 and #2 of CBD (Figure 4.2 A and B) are located out of binding sites despite the binding free energies are negative (-). There is no binding interaction was observed in this case.

#### 4.2.3. Binding Properties of CBD docked to HSA for Conf #3, #4, #5 and #6

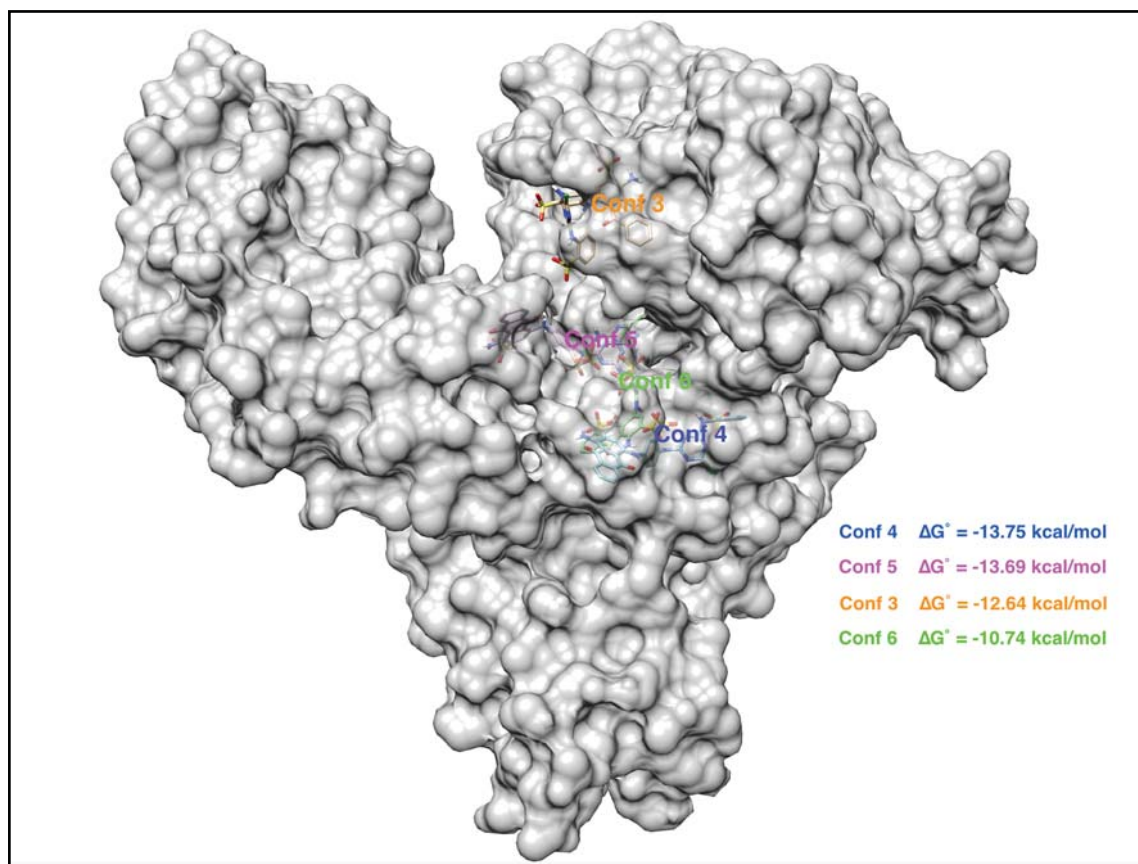
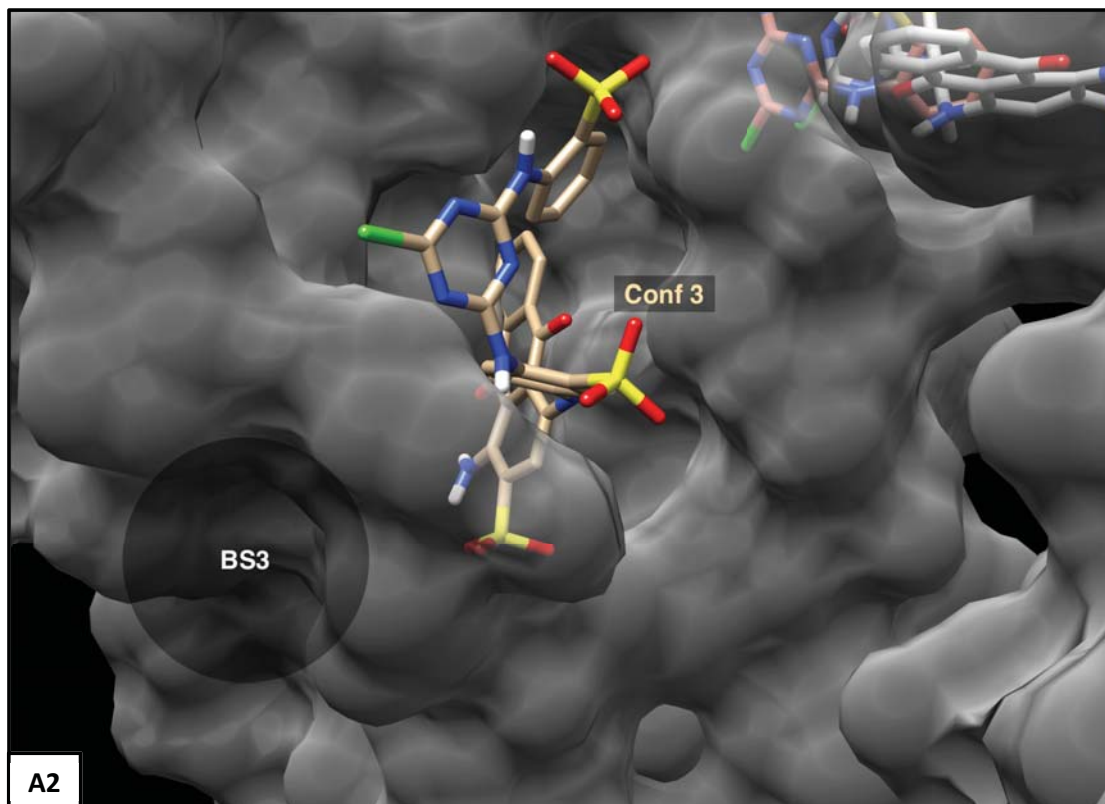
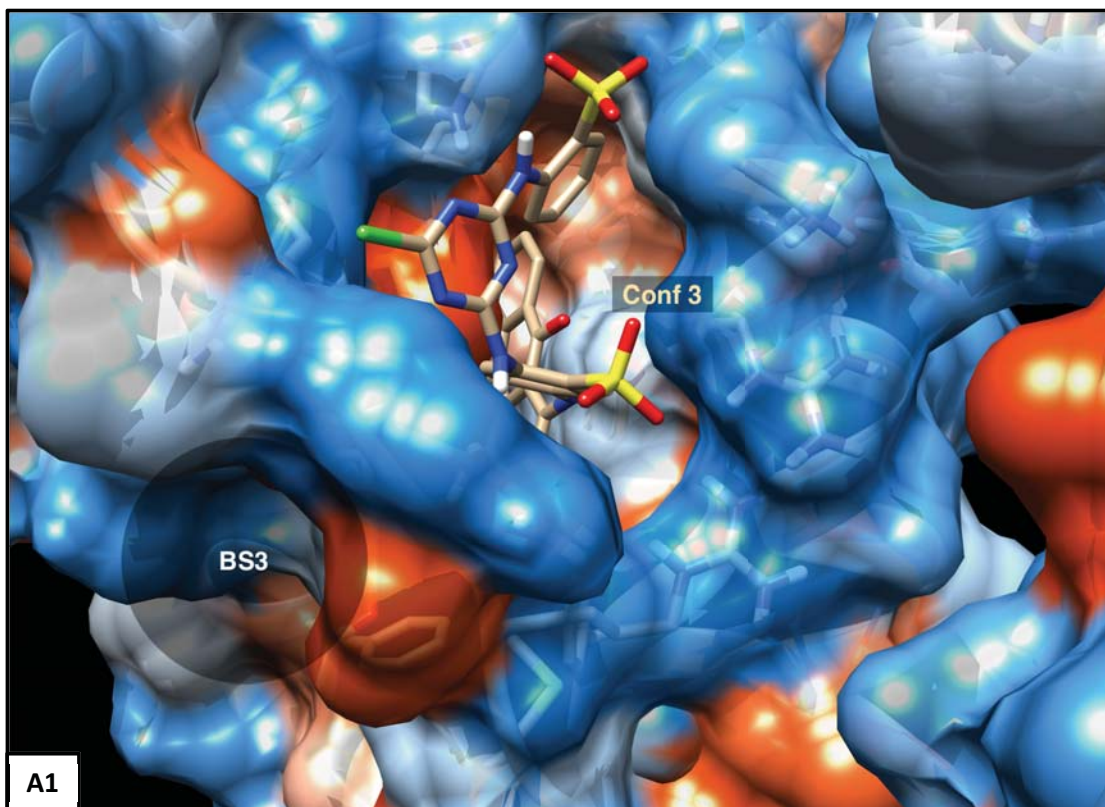


Figure 4.3. Conf 3, 4, 5, and 6 of CBD interaction with HSA (solid grey surface).

Four conformations of CBD (3,4,5 and 6) are seen in Figure 4.3 with their binding free energies. They are located in different binding sites of HSA. In Figure 4.3; Conf #4 and #6 are located at binding site 1 (BS1) of HSA, Conf #5 located at binding site 2 (BS2), namely Sudlow's site (Figure 2.3) and Conf #3 located at binding site 3 (BS3). All four conformations are energetically favorable.

#### 4.2.3.1. Binding Properties of Conf #3 and #4



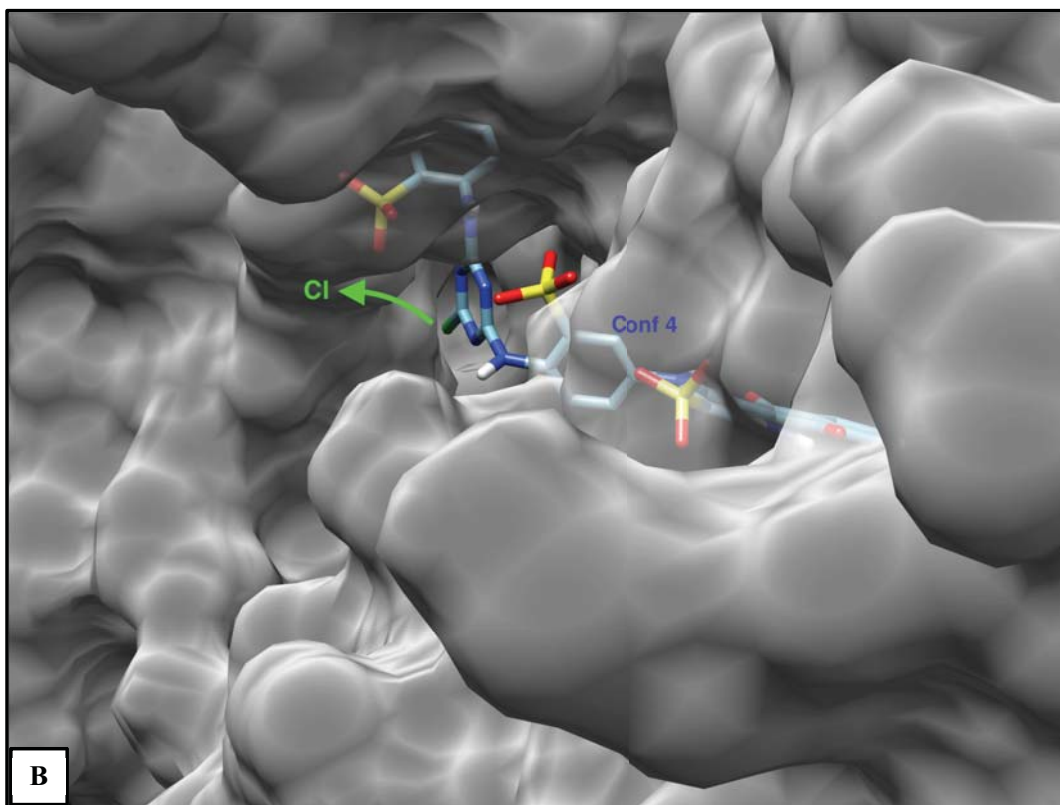


Figure 4.4. **A1)** Conformation 3 of CBD interaction with HSA (interactive hydrophobicity of solid surface). **A2)** Conformation 3 of CBD interaction with HSA (dark grey solid surface). **B)** Conformation 4 of CBD interaction with HSA (dark grey solid surface).

Figure 4.4 represents the Conf #3 and #4 of CBD molecule in complex with HSA. As seen in Figure 4 A1 and A2, Conf #3 of CBD located around BS3 of HSA, where the molecules such as hemin, bilirubin, fusicid acid, and lidocaine can also bind in this site (Figure 2.3). Figure 4 A1 particularly shows the interaction profile of Conf #3 of CBD with HSA seems both from hydrophilic and hydrophobic sites of protein through sulfonic acid and anthraquinone moiety of CBD, respectively.

Furthermore, the chloride atom (Cl) colored as the bright green oriented outer side of HSA, which means that Conf #3 of CBD is well fitted to HSA since CBD ligand should be covalently immobilized to magnetic polymers through Cl atom by a substitution reaction. In terms of thermodynamic parameters such as binding free energy, Conf #3 of CBD docking to HSA is energetically favorable with a binding free energy of -12.64 kcal/mol.

On the other hand, Figure 4B represents Conf #4 of CBD in complex with HSA, which is illustrated in dark grey solid surface. Conf #4 of CBD is located around BS1 of HSA, where different drugs can also bind this site such as thyroxine, warfarin, and indomethacin. Although the binding mode of Conf #4 of CBD is energetically most favorable among the other conformations (-13.75 kcal/mol), the Cl atom is aligned to the inner face of the protein which means that binding mode of Conf #4 of CBD to HSA is impossible due to the steric hindrance of magnetic polymer. So, it can be concluded from this result; there is no binding to HSA in Conf #4.

#### **4.2.3.2. Binding Properties of Conf #5 and #6**

Figure 4.5 illustrates Conf #5 and #6 of CBD molecule in complex with HSA. Figure 4.5A and 4.5B correspond to Conf #5 and #6 of CBD that interacts with HSA in interactive hydrophobic solid surface and dark grey solid surface, respectively. As seen in Figure 4.5, Conf #5 of CBD located around BS2, while Conf #6 of CBD located around BS1 of HSA. BS2 is the binding site 2 of HSA, where the drugs such as thyroxine, ibuprofen, and diazepam can also bind in this site (Figure 2.3). These two conformations are well fitted to HSA, and their binding modes are energetically favorable. Moreover, both Cl atoms of Conf #5 and Conf #6 are aligned to the outer face of the protein, which means that binding modes of these conformations are possible (Figure 4.5B). Among Conf #5 and Conf #6, the most favorable binding energy confirms with Conf #5 (-13.69 kcal/mol), where it oriented around BS2 to HSA (See Table 4.19). From this point, the hydrogen bonding and hydrophobic interactions are considered for Conf #5 of CBD in complex with HSA.

Conf #5 of CBD, which is the most favorable one and located around BS2, contributes both hydrophobic and hydrophilic interactions with HSA. In Figure 4.5A, sulfonic acid groups of Conf #5 of CBD interact with HSA through the most hydrophilic sites of the protein, which is denoted as orange color. In addition to, anthraquinone domain of CBD docked to HSA through the most hydrophobic sites of the protein, which is denoted as dodger blue color.

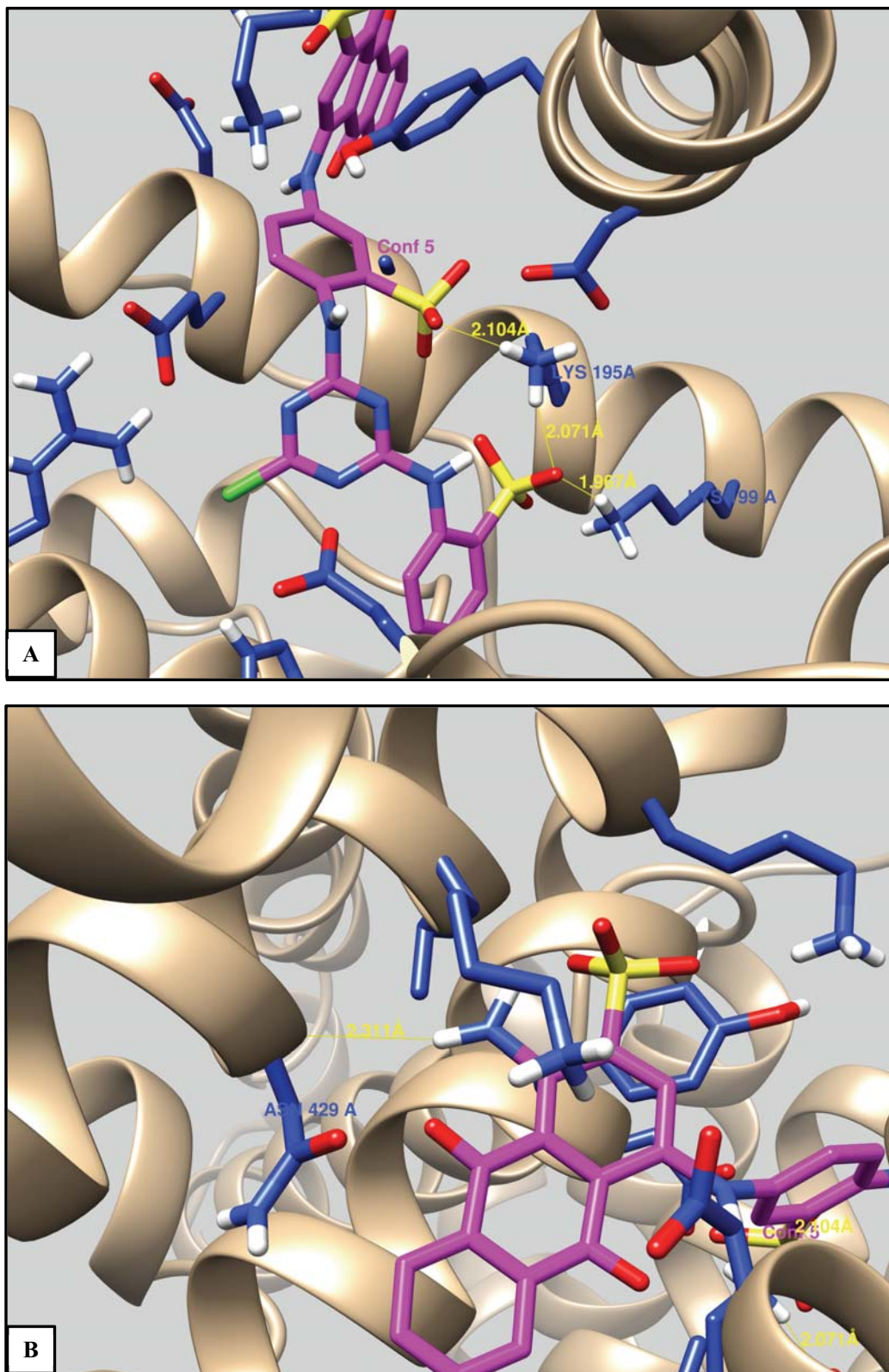


Figure 4.5. **A)** Conformation 5 and 6 of CBD interaction with HSA (interactive hydrophobicity of surface). **B)** Conformation 5 and 6 of CBD interaction with HSA (dark grey solid surface).

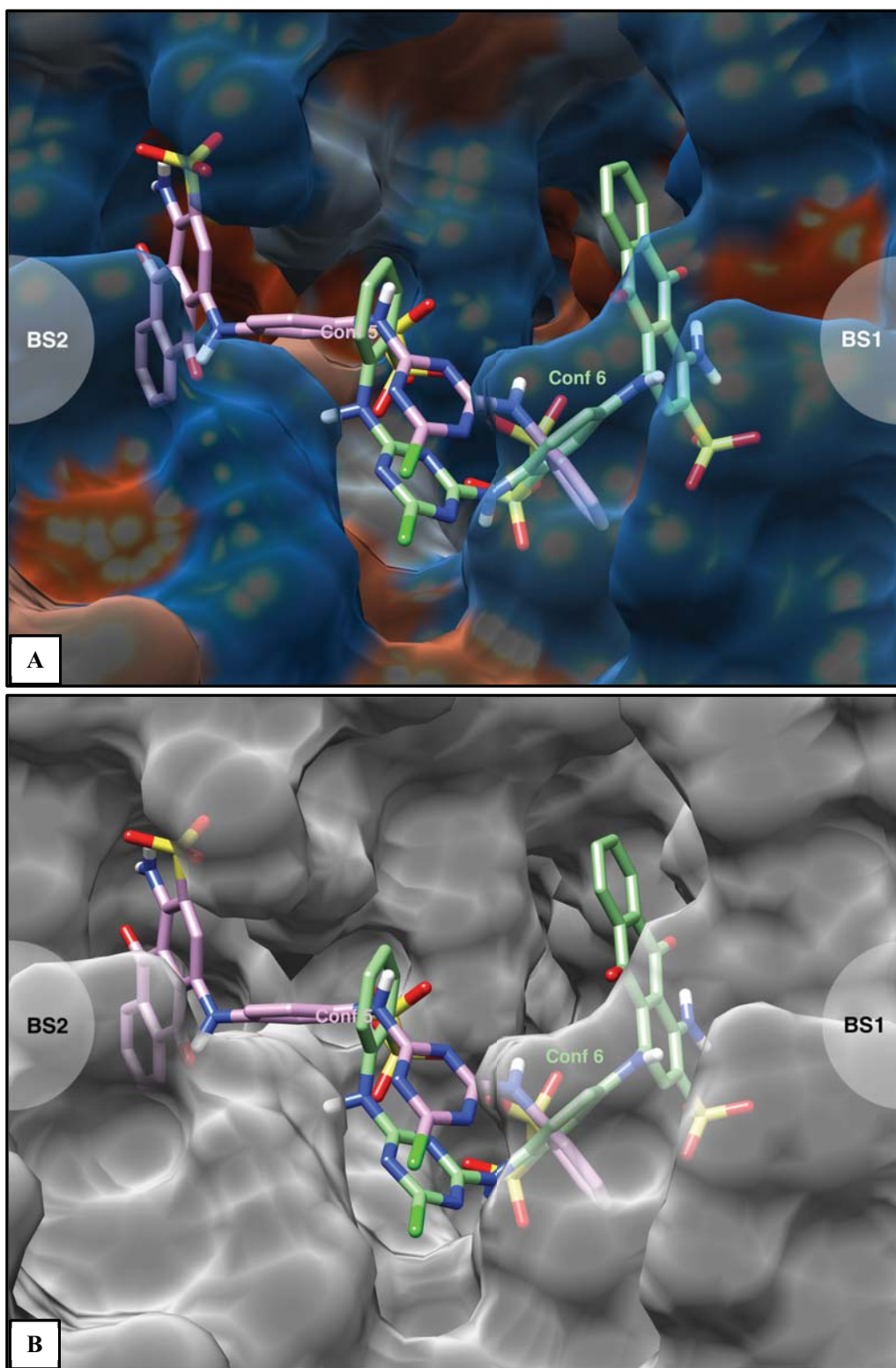


Figure 4.6. A and B) H-bonding of Conf #5 of CBD interacts with HSA (ribbon structure) in different views.

Figure 4.6 represents H-bonding interactions of Conf #5 with neighboring residues

of HSA. It is clearly seen that the sulfonic acid groups of CBD have H-bonding with LYS 195 and 199 in Domain IIIA of HSA (Figure 4.6A). In addition to, it seems an H-bonding between NH<sub>2</sub> group of CBD in anthraquinone domain and ASN 429 amino acid backbone in Domain IIIA of HSA (Figure 4.6B).

The AutoDock also analyses the specific ligand CBD interactions in a different display with neighboring amino acid residues of HSA. In Figure 4.7, the ligand is shown with a solvent-excluded molecular surface view. Atoms in the receptor which are hydrogen-bonded or in close-contact to atoms in CBD are visible as spheres. Furthermore, some pieces of the receptor are displayed for sequences of 3 or more residues in HSA which have interaction towards CBD. In this circumstance, Conf #5 is well fitted with amino acid residues of HSA.

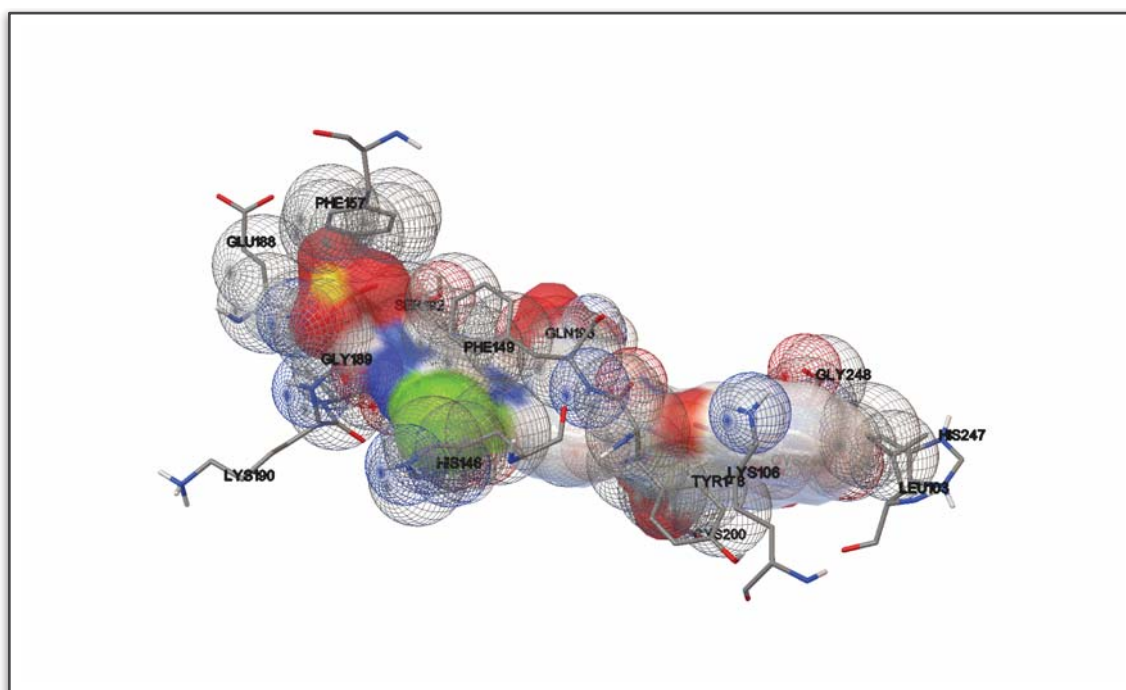


Figure 4.7. Interaction of Conf #5 of CBD with neighboring amino acid residues of HSA.



## 5.CONCLUSION

In this thesis, six different conformations of CBD in complex with HSA was evaluated by molecular docking software AutoDock v6.2 in order to investigate appreciate the molecular binding mode of CBD to HSA. Table 4.20 summarizes the binding possibilities of six conformers of CBD. Among all the conformations, Conf #5 is the most favorable one.

Table 4.20. Summary of binding features of CBD to HSA.

| Conformation # | Binding Site | Binding Energy (kcal/mol) | Binding Possibility   |
|----------------|--------------|---------------------------|-----------------------|
| 1              | --           | -9.12                     | No Binding            |
| 2              | --           | -6.08                     | No Binding            |
| 3              | BS3          | -12.64                    | Favorable             |
| 4              | BS1          | -13.75                    | No Binding            |
| <b>5</b>       | <b>BS2</b>   | <b>-13.69</b>             | <b>Most Favorable</b> |
| 6              | BS1          | -10.74                    | Favorable             |



## 6. REFERENCES

- (1) H. Ancell, Course of lectures on the physiology and pathology of the blood and other animal fluids, *Lancet*, 1 (**1839**) 222 (from the *Am. J. Dig. Dis.*, 14 (**1969**) 711-744).
- (2) M.A. Rothschild, M. Oratz, S.S. Schreiber, Serum Albumin, *Hepatology*, 2 (**1988**) 385-401.
- (3) J.D. Andrade, V. Hlady, A.P. Wei, C.G. Gölander, A domain approach to the adsorption of complex proteins: preliminary analysis and application to albumin, *Croatica Chemica Acta*, 63 (**1990**) 527-538.
- (4) X.M. He and D.C. Carter, Atomic structure and chemistry of human serum albumin, *Nature*, 358 (**1992**) 209.
- (5) T. Peters, Serum Albumin, *Adv. Protein Chem.*, 37 (**1985**) 161-245.
- (6) S. Zhang, Y. Sun, Further studies on the contribution of electrostatic and hydrophobic interactions to protein adsorption on dye-ligand adsorbents, *Biotechnol. Bioeng.*, 75 (**2001**) 710-717.
- (7) A. Denizli, E. Pişkin, Dye-ligand affinity systems, *J. Biochem. Biophys. Methods*, 49 (**2001**) 391-416.
- (8) A. Denizli, G. Köktürk, H. Yavuz, E. Pişkin, albumin adsorption from aqueous solutions and human plasma in a packed-bed column with Cibacron Blue F3GA-Zn(II) attached poly(EGDMA-HEMA) microbeads, *React. Funct. Polym.*, 40 (**1999**) 195.
- (9) N.E. Katsos, N.E. Labrou, Y.D. Clonis, Interaction of L-glutamate oxidase with triazine dyes: selection of ligands for affinity chromatography, *J. Chromatogr. B.*, 807 (**2004**) 277-285.
- (10) X. Dong, Y. Sun, Agar based magnetic affinity support for protein adsorption, *Biotechnol. Prog.*, 1 (**2001**) 738-743.
- (11) P.M. Boyer, J.T. Hsu, Protein purification by dye-ligand chromatography, *Advances in Biochemical Engineering*, 49 (**1993**) 1-44.
- (12) D. Hangghi, P. Carr, Analytical evaluation of the purity of commercial preparations of Cibacron Blue F3GA and related dyes, *Anal. Biochem.*, 149 (**1985**) 91-104.
- (13) J. Sereikate, Z. Bumeliene, V.A. Bumelis, Bovine serum albumin-dye

- binding, *Acta Chromatographica*, 15 (2005) 298-306.
- (14) R.A. Billington, J. Bak, A.M. Coscolla, M. Debidda, A.A. Genazzani, Triazine dyes are agonists of the NAADP receptor, *British J. Pharmacol.*, 142 (2004) 1231-1246.
  - (15) Y.D. Clonis, A. Atkinson, C.J. Burton, C.R. Lowe (eds) *Reactive Dyes in Protein and Enzyme Technology*, Macmillan, Basingstoke (1987).
  - (16) C.R. Lowe, in: *Topics in Enzyme and Fermentation Technology*, A. Wiseman (ed), Ellis Horwood, Chichester (1984) 78.
  - (17) C. Fields, P. Li, J.J. O'Mahony, G.U. Lee, *Advances in affinity ligand-functionalized nanomaterials for biomagnetic separation*, *Biotechnol. Bioeng.*, 113 (2016) 11-25.
  - (18) J.-C. Janson, *Protein Purification: Principles, High Resolution Methods, and Applications*, Wiley, 2011.
  - (19) I. Safarik, M. Safarikova, *Magnetic techniques for the isolation and purification of proteins and peptides*, *BioMagn. Res. Technol.*, 2, Article No. 7 (2004) 1-17.
  - (20) S. Ji, N. Li, Y. Shen, Q. Li, J. Qiao, Z. Li, *Poly(amino acid)-based thermoresponsive molecularly imprinted magnetic nanoparticles for specific recognition and release of lysozyme*, *Anal. Chim. Acta*, 909 (2016) 60-66.
  - (21) P. Fraga García, M. Brammen, M. Wolf, S. Reinlein, M. Freiherr von Roman, S. Berensmeier, *High-gradient magnetic separation for technical scale protein recovery using low cost magnetic nanoparticles*, *Sep. Purif. Technol.*, 150 (2015) 29-36.
  - (22) H. Nirschl, K. Kelle, *Upscaling of bio-nano-processes. Selective bioseparation by magnetic particles*, *Lecture Notes in Bioengineering*, Springer-Verlag Berlin Heidelberg, (2014) 245.
  - (23) G. Bayramoglu, V.C. Ozalp, B. Altintas, M.Y. Arica, *Preparation and characterization of mixed-mode magnetic adsorbent with p-amino-benzamidine ligand: Operated in a magnetically stabilized fluidized bed reactor for purification of trypsin from bovine pancreas*, *Process Biochem.*, 49 (2014) 520-528.
  - (24) S. Flygare, P. Wikstrom, G. Johansson, P.O. Larsson, *Magnetic aqueous two-phase separation in preparative applications*, *Enzyme Microb. Technol.*, 12 (1990) 95-103.

- (25) I. Yildiz, Applications of magnetic nanoparticles in biomedical separation and purification, *Nanotechnol. Rev.*, 5 (2016) 331-340.
- (26) M. Iranmanesh, J. Hulliger, Magnetic separation: its application in mining, waste purification, medicine, biochemistry and chemistry, *Chem. Soc. Rev.*, 46 (2017) 5925-5934.
- (27) C.T. Yavuz, A. Prakash, J.T. Mayo, V.L. Colvin, Magnetic separations: From steel plants to biotechnology, *Chem. Eng. Sci.*, 64 (2009) 2510-2521.
- (28) S. Elingarami, X. Zeng, A short review on current use of magnetic nanoparticles for bio-separation, sequencing, diagnosis and drug delivery, *Adv. Sci. Lett.*, 4 (2011) 3295-3300.
- (29) L. Borlido, A.M. Azevedo, A.C.A. Roque, M.R. Aires-Barros, Magnetic separations in biotechnology, *Biotechnol. Adv.*, 31 (2013) 1374-1385.
- (30) I. Safarik, K. Horska, L.M. Martinez, M. Safarikova, Large scale magnetic separation of *Solanum tuberosum* tuber lectin from potato starch waste water, *AIP Conf Proc.*, 1311 (2010) 146-151.
- (31) J.J. Hubbuch, O.R.T. Thomas, High-gradient magnetic affinity separation of trypsin from porcine pancreatin, *Biotechnol. Bioeng.*, 79 (2002) 301-313.
- (32) S. Laurent, D. Forge, M. Port, A. Roch, C. Robic, L.V. Elst, R.N. Muller, Magnetic iron oxide nanoparticles: Synthesis, stabilization, vectorization, physicochemical characterizations, and biological applications, *Chem. Rev.*, 108 (2008) 2064-2110.
- (33) Y. Li, X. Zhang, C. Deng, Functionalized magnetic nanoparticles for sample preparation in proteomics and peptidomics analysis, *Chem. Soc. Rev.*, 42 (2013) 8517-8539.
- (34) S. Teotia, M.N. Gupta, Purification of  $\alpha$ -amylases using magnetic alginate beads, *Appl. Biochem. Biotechnol.*, 90 (2001) 211-220.
- (35) I. Safarik, K. Pospiskova, E. Baldikova, M. Safarikova, Magnetically responsive biological materials and their applications, *Adv. Mater. Lett.*, 7 (2016) 254-261.
- (36) I. Safarik, M. Safarikova, Magnetic affinity separation of recombinant fusion proteins, *Hacettepe J. Biol. Chem.*, 38 (2010) 1-7.
- (37) N. Li, L. Qi, Y. Shen, J. Qiao, Y. Chen, Novel oligo(ethylene glycol)-based molecularly imprinted magnetic nanoparticles for thermally modulated

- capture and release of lysozyme, *ACS Appl. Mater. Interfaces*, 6 (2014) 17289-17295.
- (38) A.S. Murphy, K.R. Hoogner, W.A. Peer, L. Taiz, Identification, purification, and molecular cloning of N-1- naphthylphthalamic acid-binding plasma membrane-associated aminopeptidases from *Arabidopsis*, *Plant Physiol.*, 128 (2002) 935-950.
- (39) M. Rajčanová, M. Tichá, Z. Kučerová, Application of heptapeptides containing D-amino acid residues immobilized to magnetic particles and Sepharose for the study of binding properties of gastric aspartic proteases, *J. Sep. Sci.*, 35 (2012) 1899-1905.
- (40) C.L. Yang, J.M. Xing, Y.P. Guan, H.Z. Liu, Superparamagnetic poly(methyl methacrylate) beads for nattokinase purification from fermentation broth, *Appl. Microb. Biotechnol.*, 72 (2006) 616-622.
- (41) M. Filuszová, Z. Kučerová, M. Tichá, Peptide inhibitor modified magnetic particles for pepsin separation, *J. Sep. Sci.*, 32 (2009) 2017-2021.
- (42) J.J. Hubbuch, D.B. Matthiesen, T.J. Hobbey, O.R.T. Thomas, High gradient magnetic separation versus expanded bed adsorption: a first principle comparison, *Bioseparation*, 10 (2001) 99-112.
- (43) M. Cerff, A. Scholz, T. Käppler, K.E. Ottow, T.J. Hobbey, C. Posten, Semi-continuous in situ magnetic separation for enhanced extracellular protease production—modeling and experimental validation, *Biotechnol. Bioeng.*, 110 (2013) 2161-2172.
- (44) T.L. Maury, K.E. Ottow, J. Brask, J. Villadsen, T.J. Hobbey, Use of high-gradient magnetic fishing for reducing proteolysis during fermentation, *Biotechnol. J.*, 7 (2012) 909-918.
- (45) C.L. Yang, Y.P. Guan, J.M. Xing, H.Z. Liu, Development of superparamagnetic functional carriers and application for affinity separation of subtilisin Carlsberg, *Polymer*, 47 (2006) 2299-2304.
- (46) M. Goto, T. Imamura, T. Hirose, S. Motoyuki, Purification of enzyme by affinity separation with magnetic adsorbent, *Studies Surface Sci. Catal.*, 80 (1993) 227-234.
- (47) P.J. Halling, P. Dunnill, Recovery of free enzymes from product liquors by bio-affinity adsorption: Trypsin binding by immobilised soybean inhibitor, *Eur. J. Appl. Microbiol.*, 6 (1979) 195-205.

- (48) X.N. An, Z.X. Su, Characterization and application of high magnetic property chitosan particles, *J. Appl. Polym. Sci.*, 81 (2001) 1175-1181.
- (49) Y.S. Dong, F. Liang, X.Y. Yu, J.H. Chang, L.A. Guo, Preparation of novel magnetic dextran affinity adsorbents and their application to purify urokinase, *Chinese J. Chromatogr.*, 19 (2001) 21-24.
- (50) Y.S. Dong, F. Liang, X.Y. Yu, J.H. Chang, L.A. Guo, A study on magnetic agarose affinity adsorbents for the purification of urokinase, *J. Northwest Univ.*, 31 (2001) 121-123.
- (51) X.D. Tong, B. Xue, Y. Sun, A novel magnetic affinity support for protein adsorption and purification, *Biotechnol. Prog.*, 17 (2001) 134-139.
- (52) N. Kaya, D.A. Uygun, S. Akgol, A. Denizli, Purification of alcohol dehydrogenase from *Saccharomyces cerevisiae* using magnetic dye-ligand affinity nanostructures, *Appl. Biochem. Biotechnol.*, 169 (2013) 2153-2164.
- (53) S.A. Ghotb, M. Chamani, H. Ahmadpanahi, A.A. Sadeghi, Clarified rumen fluid as a source of cellulase extraction by Cibacron Blue coated magnetic nanoparticles, *Onl. J. Vet. Res.*, 19 (2015) 306-316.
- (54) M.P. Ennis, G.B. Wisdom, A magnetizable solid phase for enzyme extraction, *Appl. Biochem. Biotechnol.*, 30 (1991) 155-164.
- (55) N. Basar, L. Uzun, A. Guner, A. Denizli, Lysozyme purification with dye-affinity beads under magnetic field, *Int. J. Biol. Macromol.*, 41 (2007) 234-242.
- (56) Z. Li, M. Cao, W. Zhang, L. Liu, J. Wang, W. Ge, Y. Yuan, T. Yue, R. Li, W.W. Yu, Affinity adsorption of lysozyme with Reactive Red 120 modified magnetic chitosan microspheres, *Food Chem.*, 145 (2014) 749-755.
- (57) M. Odabasi, A. Denizli, Cibacron blue F3GA incorporated magnetic poly(2-hydroxyethyl methacrylate) beads for lysozyme adsorption, *J. Appl. Polym. Sci.*, 93 (2004) 719-725.
- (58) X.D. Tong, Y. Sun, Application of magnetic agarose support in liquid magnetically stabilized fluidized bed for protein adsorption, *Biotechnol. Prog.*, 19 (2003) 1721-1727.
- (59) Y.H. Yu, B. Xue, Y. Sun, B.L. He, The preparation of chitosan affinity magnetic nanoparticles and their adsorption properties for proteins, *Acta Polym. Sin.*, 3 (2000) 340-344.

- (60) N.A. Ghazvini, M. Chamani, H.A. Panahi, A.A. Sadeghi, M. Aminafshar, Sorption of ruminal fluid derived phytase onto modified nanoparticles and determination of its desorption capacity, *Int. J. Biosci.*, 5 (2014) 250-257.
- (61) H. Farzi-Khajeh, K.D. Safa, S. Dastmalchi, Arsanilic acid modified superparamagnetic iron oxide nanoparticles for purification of alkaline phosphatase from hen's egg yolk, *J. Chromatogr. B*, 1061-1062 (2017) 26-33.
- (62) M.C. Wu, J. Lin, S.T. Kuo, Y. Lin, Purification of amylase from Tilapia by magnetic particle, *J. Food Process. Preserv.*, 34 (2010) 139-151.
- (63) P. Dunnill, M.D. Lilly, Purification of enzymes using magnetic bio-affinity materials, *Biotechnol. Bioeng.*, 16 (1974) 987-990.
- (64) Z.A. Lin, J.N. Zheng, F. Lin, L. Zhang, Z.W. Cai, G.N. Chen, Synthesis of magnetic nanoparticles with immobilized aminophenylboronic acid for selective capture of glycoproteins, *J. Mater. Chem.*, 21 (2011) 518-524.
- (65) K. Nishio, Y. Masaike, M. Ikeda, H. Narimatsu, N. Gokon, S. Tsubouchi, M. Hatakeyama, S. Sakamoto, N. Hanyu, A. Sandhu, H. Kawaguchi, M. Abe, H. Handa, Development of novel magnetic nano-carriers for high-performance affinity purification, *Colloid. Surf. B: Biointerfaces*, 64 (2008) 162-169.
- (66) C.S.M. Fernandes, R. dos Santos, S. Ottengy, A.C. Viecinski, G. Béhar, B. Mouratou, F. Pecorari, A.C.A. Roque, Affitins for protein purification by affinity magnetic fishing, *J. Chromatogr. A*, 1457 (2016) 50-58.
- (67) E.B. Altıntaş, N. Tüzmen, N. Candan, A. Denizli, Use of magnetic poly(glycidyl methacrylate) monosize beads for the purification of lysozyme in batch system, *J. Chromatogr. B*, 853 (2007) 105-113.
- (68) C.-H. Liu, H.-Y. Lai, W.-C. Wu, Facile synthesis of magnetic iron oxide nanoparticles for nattokinase isolation, *Food Bioproducts Process.*, 102 (2017) 260-267.
- (69) Z.Q. Samra, S. Shabir, Z. Rehmat, M. Zaman, A. Nazir, N. Dar, M.A. Athar, Synthesis of cholesterol-conjugated magnetic nanoparticles for purification of human paraoxonase 1, *Appl. Biochem. Biotechnol.*, 162 (2010) 671-686.
- (70) M. Pan, Y. Sun, J. Zheng, W. Yang, Boronic acid-functionalized core-shell-shell magnetic composite microspheres for the selective enrichment of glycoprotein, *ACS Appl. Mater. Interfaces*, 5 (2013) 8351-8358.



- (71) K. Sparbier, S. Koch, I. Kessler, T. Wenzel, M. Kostrzewa, Selective isolation of glycoproteins and glycopeptides for MALDI-TOF MS detection supported by magnetic particles, *J. Biomolec. Techniques*, 16 (2005) 407-413.
- (72) J.H. Lee, Y.S. Kim, M.Y. Ha, E.K. Lee, J.B. Choo, Immobilization of aminophenylboronic acid on magnetic beads for the direct determination of glycoproteins by matrix assisted laser desorption ionization mass spectrometry, *J. Am. Soc. Mass Spectr.*, 16 (2005) 1456-1460.
- (73) M.H.M.E. Alves, G.A. Nascimento, M.P. Cabrera, S.I.D. Silveri, C. Nobre, J.A. Teixeira, L.B. de Carvalho, Trypsin purification using magnetic particles of azocasein-iron composite, *Food Chem.*, 226 (2017) 75-78.
- (74) T. Paul, S. Chatterjee, A. Bandyopadhyay, D. Chattopadhyay, S. Basu, K. Sarkar, A simple one pot purification of bacterial amylase from fermented broth based on affinity toward starch-functionalized magnetic nanoparticle, *Preparat. Biochem. Biotechnol.*, 45 (2015) 501-514.
- (75) M. Safarikova, I. Roy, M.N. Gupta, I. Safarik, Magnetic alginate microparticles for purification of  $\alpha$ -amylases, *J. Biotechnol.*, 105 (2003) 255-260.
- (76) S. Teotia, M.N. Gupta, Magnetite-alginate beads for purification of some starch degrading enzymes, *Mol. Biotechnol.*, 20 (2002) 231-237.
- (77) D. Spanò, K. Pospiskova, I. Safarik, M.B. Pisano, F. Pintus, G. Floris, R. Medda, Chitinase III in *Euphorbia characias* latex: Purification and characterization, *Protein Expr. Purif.*, 116 (2015) 152-158.
- (78) S. Martos, D. Spanò, N. Agustí, C. Poschenrieder, F. Pintus, L. Moles, R. Medda, A chitinase from *Euphorbia characias* latex is a novel and powerful plant-based pesticide against *Drosophila suzukii*, *Ann. Appl. Biol.*, 171 (2017) 252-263.
- (79) M. Safarikova, K. Horska, Z. Maderova, A. Tonkova, V. Ivanova-Pashkoulova, I. Safarik, Magnetic porous corn starch for the affinity purification of cyclodextrin glucanotransferase produced by *Bacillus circulans*, *Biocatal. Biotransform.*, 30 (2012) 96-101.
- (80) I. Safarik, Magnetic biospecific affinity adsorbents for lysozyme isolation, *Biotechnol. Techniques*, 5 (1991) 111-114.
- (81) I. Safarik, M. Safarikova, Batch isolation of hen egg white lysozyme with magnetic chitin, *J. Biochem. Biophys. Methods*, 27 (1993) 327-330.

- (82) I. Safarik, M. Safarikova, F. Weyda, E. Mosiniewicz-Szablewska, A. Slawska-Waniewska, Ferrofluid-modified plant-based materials as adsorbents for batch separation of selected biologically active compounds and xenobiotics, *J. Magn. Magn. Mater.*, 293 (2005) 371-376.
- (83) P. Kopacek, R. Vogt, L. Jindrak, C. Weise, I. Safarik, Purification and characterization of the lysozyme from the gut of the soft tick *Ornithodoros moubata*, *Insect Biochem. Molec. Biol.*, 29 (1999) 989-997.
- (84) R. Tyagi, M.N. Gupta, Purification and immobilization of *Aspergillus niger* pectinase on magnetic latex beads, *Biocatal. Biotransform.*, 12 (1995) 293-298.
- (85) A. Frenzel, C. Bergemann, G. Kohl, T. Reinard, Novel purification system for 6xHis-tagged proteins by magnetic affinity separation, *J. Chromatogr. B*, 793 (2003) 325-329.
- (86) J. Bao, W. Chen, T.T. Liu, Y.L. Zhu, P.Y. Jin, L.Y. Wang, J.F. Liu, Y.G. Wei, Y.D. Li, Bifunctional Au-Fe<sub>3</sub>O<sub>4</sub> nanoparticles for protein separation, *ACS Nano*, 1 (2007) 293-298.
- (87) L. Skarydova, R. Andrys, L. Holubova, H. Stambergova, J. Knavova, V. Wsol, Z. Bilkova, Efficient isolation of carbonyl-reducing enzymes using affinity approach with anticancer drug oracin as a specific ligand, *J. Sep. Sci.*, 36 (2013) 1176-1184.
- (88) Y. Zhang, Y. Yang, W. Ma, J. Guo, Y. Lin, C. Wang, Uniform magnetic core/shell microspheres functionalized with Ni<sup>2+</sup>-iminodiacetic acid for one step purification and immobilization of His-tagged enzymes, *ACS Appl. Mater. Interfaces*, 5 (2013) 2626-2633.
- (89) P.-C. Lin, C.-C. Yu, H.-T. Wu, Y.-W. Lu, C.-L. Han, A.-K. Su, Y.-J. Chen, C.-C. Lin, A chemically functionalized magnetic nanoplatfrom for rapid and specific biomolecular recognition and separation, *Biomacromolecules*, 14 (2013) 160-168.
- (90) T. Belien, S. Van Campenhout, M. Van Acker, G. Volckaert, Cloning and characterization of two endoxylanases from the cereal phytopathogen *Fusarium graminearum* and their inhibition profile against endoxylanase inhibitors from wheat, *Biochem. Biophys. Res. Commun.*, 327 (2005) 407-414.
- (91) J. Meng, J.G. Walter, O. Kokpinar, F. Stahl, T. Scheper, Automated microscale His-tagged protein purification using Ni-NTA magnetic agarose

- beads, Chem. Eng. Technol., 31 (2008) 463-468.
- (92) L. Qiao, B. Lv, X. Feng, C. Li, A new application of aptamer: One-step purification and immobilization of enzyme from cell lysates for biocatalysis, J. Biotechnol., 203 (2015) 68-76.
- (93) M.W. Fuellgrabe, K. Boonrod, R. Jamous, M. Moser, Y. Shibolet, G. Krczal, M. Wassenegger, Expression, purification and functional characterization of recombinant Zucchini yellow mosaic virus HC-Pro, Protein Express. Purif., 75 (2011) 40-45.
- (94) J.J. Wu, L.L. Zhou, H.J. Zhang, J. Guo, X. Mei, C. Zhang, J.Y. Yuan, X.H. Xing, Direct affinity immobilization of recombinant heparinase I fused to maltose binding protein on maltose-coated magnetic nanoparticles, Biochem. Eng. J., 90 (2014) 170-177.
- (95) Y. Nishiya, T. Hibi, J.L. Oda, A purification method of the diagnostic enzyme *Bacillus* uricase using magnetic beads and non-specific protease, Protein Express. Purif., 25 (2002) 426-429.
- (96) X. Xu, R. Liu, P. Guo, Z. Luo, X. Cai, H. Shu, Y. Ge, C. Chang, Q. Fu, Fabrication of a novel magnetic mesoporous molecularly imprinted polymer based on pericarpium granati-derived carrier for selective absorption of bromelain, Food Chem., 256 (2018) 91-97.
- (97) Q.Q. Gai, F. Qu, Z.J. Liu, R.J. Dai, Y.K. Zhang, Superparamagnetic lysozyme surface-imprinted polymer prepared by atom transfer radical polymerization and its application for protein separation, J. Chromatogr. A, 1217 (2010) 5035-5042.
- (98) T. Jing, H.R. Du, Q. Dai, H.A. Xia, J.W. Niu, Q.L. Hao, S.R. Mei, Y.K. Zhou, Magnetic molecularly imprinted nanoparticles for recognition of lysozyme, Biosens. Bioelectron., 26 (2010) 301-306.
- (99) Y. Wang, Z. Chai, Y. Sun, M. Gao, G. Fu, Preparation of lysozyme imprinted magnetic nanoparticles via surface graft copolymerization, J. Biomater. Sci., Polym. Ed., 26 (2015) 644-656.
- (100) H. Guo, D. Yuan, G. Fu, Enhanced surface imprinting of lysozyme over a new kind of magnetic chitosan submicrospheres, J. Colloid Interface Sci., 440 (2015) 53-59.
- (101) J. Cao, X. Zhang, X. He, L. Chen, Y. Zhang, The synthesis of magnetic lysozyme-imprinted polymers by means of distillation-precipitation

- polymerization for selective protein enrichment, *Chemistry – Asian J.*, 9 (2014) 526-533.
- (102) T. Jing, H. Xia, Q. Guan, W. Lu, Q. Dai, J. Niu, J.-M. Lim, Q. Hao, Y.-I. Lee, Y. Zhou, S. Mei, Rapid and selective determination of urinary lysozyme based on magnetic molecularly imprinted polymers extraction followed by chemiluminescence detection, *Anal. Chim. Acta*, 692 (2011) 73-79.
- (103) R. Rohs, I. Bloch, H. Sklenar, Z. Shakked, Molecular flexibility in ab-initio drug docking to DNA: binding-site and binding-mode transitions in all-atom Monte Carlo simulations, *Nucl. Acids Res.*, 33 (2005) 7048-7057.
- (104) I.A. Guedes IA, C.S. de Magalhães, L.E. Dardenne, Receptor-ligand molecular docking, *Biophys. Rev.*, 6 (2014) 75-87.
- (105) S. Agarwal, D. Chadha, R. Mehrotra, Molecular modeling and spectroscopic studies of semustine binding with DNA and its comparison with lomustine–DNA adduct formation, *J. Biomol. Struct. Dyn.*, 33 (2015) 1653-1668.
- (106) S.Y. Huang, Z. Xiaoqin, Advances and challenges in protein-ligand docking, *Int. J. Mol. Sci.*, 11 (2010) 3016-3034.
- (107) S.F. Sousa, P.A. Fernandes, M.J. Ramos, Protein–ligand docking: current status and future challenges, *Proteins: Structure, Function, and Bioinformatics* 65.1 (2006) 15-26.
- (108) Molecular modelling from Wikipedia, the free encyclopedia [https://en.wikipedia.org/wiki/Molecular\\_modelling](https://en.wikipedia.org/wiki/Molecular_modelling) (Accessed on June 17, 2019)
- (109) R. Wang, X. Fang, Y. Lu, S.Y. Yang, S. Wang, The PDBbind database: methodologies and updates, *J. Med. Chem.*, 48 (2005) 4111-4119.
- (110) D. Puvanendrapillai, J.B.O. Mitchell, Protein ligand database (PLD): additional understanding of the nature and specificity of protein–ligand complexes, *Bioinformatics* 19 (2003) 1856-1857.
- (111) P. Block, C.A. Sotriffer, I. Dramburg, G. Klebe, AffinDB: a freely accessible database of affinities for protein–ligand complexes from the PDB, *Nucl. Acids Res.*, 34 (2006) 522-526.
- (112) T. Liu, et al., Binding DB: a web-accessible database of experimentally determined protein–ligand binding affinities, *Nucleic Acids Research*, 35 (2007) 198-201.
- (113) R.D. de Azevedo, F. Walter, Molecular docking algorithms, *Current Drug*

- Targets, 9 (2008) 1040-1047.
- (114) Morris, G. M., Huey, R., Lindstrom, W., Sanner, M. F., Belew, R. K., Goodsell, D. S. and Olson, A. J. Autodock4 and AutoDockTools4: automated docking with selective receptor flexibility. *J. Computational Chemistry*, 16 (2009) 2785-2791.
- (115) UCSF Chimera--a visualization system for exploratory research and analysis. Pettersen EF, Goddard TD, Huang CC, Couch GS, Greenblatt DM, Meng EC, Ferrin TE. *J Comput Chem*. 2004 Oct;25,13, (2004) 1605-1612.
- (116) UCSF Chimera Home Page, <https://www.cgl.ucsf.edu/chimera/> (Accessed on June 17, 2019)
- (117) R. Salomon-Ferrer, D.A. Case, R.C. Walker. An overview of the Amber biomolecular simulation package. *WIREs Comput. Mol. Sci.* 3, (2013) 198-210.
- (118) Antechamber, <http://ambermd.org/antechamber/ac.html>, (Accessed on June 17, 2019)
- (119) The Molecular Modeling Toolkit, <http://dirac.cnrs-orleans.fr/MMTK/> (Accessed on June 17, 2019)
- (120) Raquel dos Santos, Carina Figueiredo, Aline Canani Viacinski, Ana Sofia Pina, Arménio J.M. Barbosa, A. Cecília A. Roque, Designed affinity ligands to capture human serum albumin, *Journal of Chromatography A*, 1583 (2019) 88-97, <https://doi.org/10.1016/j.chroma.2018.11.021>.
- (121) J. Curling, N. Goss, J. Bertolini, in: J. Bertolini, N. Goss, J. Curling (Eds.), *Production of Plasma Proteins for Therapeutic Use*, John Wiley & Sons, Inc, Hoboken, NJ, USA, 2012.
- (122) B. Elsadek, F. Kratz, Impact of albumin on drug delivery — new applications on the horizon, *J. Control. Release* 157 (2012) 4–28, <http://dx.doi.org/10.1016/j.jconrel.2011.09.069>.
- (123) Market Research Bureau Inc, *The Worldwide Plasma Proteins Market*, 2014.
- (124) T. Burnouf, Integration of chromatography with traditional plasma protein fractionation methods, *Bioseparation* 1 (1991) 383–396.
- (125) Y. He, T. Ning, T. Xie, Q. Qiu, L. Zhang, Y. Sun, D. Jiang, K. Fu, F. Yin, W. Zhang, L. Shen, H. Wang, J. Li, Q. Lin, Y. Sun, H. Li, Y. Zhu, D. Yang,

- Large-scale production of functional human serum albumin from transgenic rice seeds, *Proc. Natl. Acad. Sci.* 108 (2011) 19078–19083, <http://dx.doi.org/10.1073/pnas.1109736108>.
- (126) M. Belew, M. Li, Yan, Zhang, K. Wei, Caldwell, Purification of recombinant human serum albumin (rHSA) produced by genetically modified *Pichia pastoris*, *Sep. Sci. Technol.* 43 (2008) 3134–3153, <http://dx.doi.org/10.1080/01496390802221857>.
- (127) E.J. Cohn, The properties and functions of the plasma proteins, with a consideration of the methods for their separation and purification, *Chem. Rev.* 28 (1941) 395–417, <http://dx.doi.org/10.1021/cr60090a007>.
- (128) Kine Marita Knudsen Sand, Malin Bern, Jeannette Nilsen, HannaTheodora Noordzij, Inger Sandlie and Jan Terje Andersen, Unraveling the interaction between FcRn and albumin: opportunities for design of albumin-based therapeutics, *Frontiers in Immunology*, 5 (2015) 682.
- (129) J. Travis, J. Bowen, D. Tewksbury, D. Johnson, R. Pannell, Isolation of albumin from whole human plasma and fractionation of albumin-depleted plasma, *Biochem. J.* 157 (1976) 301–306.
- (130) T. Burnouf, M. Radosevich, Affinity chromatography in the industrial purification of plasma proteins for therapeutic use, *J. Biochem. Biophys. Methods* 49 (2001) 575–586, [http://dx.doi.org/10.1016/S0165-022X\(01\)00221-4](http://dx.doi.org/10.1016/S0165-022X(01)00221-4).
- (131) D. Hanggi, P. Carr, Analytical evaluation of the purity of commercial preparations of Cibacron Blue F3GA and related dyes, *Anal. Biochem.* 149 (1985) 91–104.
- (132) C.R. Lowe, Combinatorial approaches to affinity chromatography, *Curr. Opin. Chem. Biol.* 5 (2001) 248–256, [http://dx.doi.org/10.1016/S1367-5931\(00\)00199-X](http://dx.doi.org/10.1016/S1367-5931(00)00199-X).
- (133) A.C.A. Roque, C.R. Lowe, Rationally designed ligands for use in affinity chromatography: an artificial protein L, in: M. Zachariou (Ed.), *Methods Mol. Biol.*, Second, Humana Press, Totowa, NJ, (2008) 93–109, [http://dx.doi.org/10.1007/978-1-59745-582-4\\_7](http://dx.doi.org/10.1007/978-1-59745-582-4_7).
- (134) I.L. Batalha, A. Hussain, A.C.A. Roque, Gum Arabic coated magnetic nanoparticles with affinity ligands specific for antibodies, *J. Mol. Recognit.* 23 (2010) 462–471, <http://dx.doi.org/10.1002/jmr.1013>.

- (135) V.L. Dhadge, P.I. Morgado, F. Freitas, M.A. Reis, A. Azevedo, R. Aires-Barros, A.C.A. Roque, An extracellular polymer at the interface of magnetic bioseparations, *J. R. Soc. Interface*, 20140743, (2014) 1-11. <http://dx.doi.org/10.1098/rsif.2014.0743>.
- (136) K. Sproule, P. Morrill, J.C. Pearson, S.J. Burton, K.R. Hejnaes, H. Valore, S. Ludvigsen, C.R. Lowe, New strategy for the design of ligands for the purification of pharmaceutical proteins by affinity chromatography, *J. Chromatogr. B Biomed. Sci. Appl.* 740 (2000) 17–33, [http://dx.doi.org/10.1016/S0378-4347\(99\)00570-8](http://dx.doi.org/10.1016/S0378-4347(99)00570-8).
- (137) C.S.M. Fernandes, R. Castro, A. Sofia, A.C.A. Roque, Small synthetic ligands for the enrichment of viral particles pseudotyped with amphotropic murine leukemia virus envelope, *J. Chromatogr. A* 1438 (2016) 160–170, <http://dx.doi.org/10.1016/j.chroma.2016.02.026>.
- (138) 1QRD, <https://rcsb.org/structure/1qrd> , DOI: 10.2210/pdb1QRD/pdb (Accessed on June 17, 2019)
- (139) C.A. Andac, Muge Andac, Adil Denizli, Predicting the binding properties of cibacron blue F3GA in affinity separation systems, *International Journal of Biological Macromolecules* 41 (2007) 430–438
- (140) 2BXQ, <https://rcsb.org/structure/2bxq>, DOI: 10.2210/pdb2BXQ/pdb (Accessed on June 17, 2019)
- (141) UCSF Chimera Usage, <https://www.cgl.ucsf.edu/chimera/docs/UsersGuide/midas/minimize.html> (Accessed on June 17, 2019)
- (142) Shapovalov, M.S., and Dunbrack, R.L., Jr., A Smoothed Backbone-Dependent Rotamer Library for Proteins Derived from Adaptive Kernel Density Estimates and Regressions Structure, 19 (2011) 844-858.
- (143) Automatic atom type and bond type perception in molecular mechanical calculations. Wang J, Wang W, Kollman PA, Case DA. *J Mol Graph Model.* 2 (2006) 247.
- (144) Sergio Mares-Sámamo, Ramón Garduño-Juárez, Computational Modeling of the Interactions of Drugs with Human Serum Albumin (HSA), *Computación y Sistemas*, Vol. 22, No. 4, (2018) 1123–1135 doi: 10.13053/CyS-22-4-3085
- (145) Omar Deeb, Martha Cecilia Rosales-Hernández, Carlos Gómez-Castro, Ramón Garduño-Juárez, José Correa-Basurto, Exploration of Human Serum Albumin Binding Sites by Docking and Molecular Dynamics Flexible

Ligand–Protein Interactions, Biopolymers Volume 93, Issue 2, (2010)  
161-170. DOI 10.1002/bip.21314



## **APPENDIX**

### **APPENDIX 1 - Originality Report**



HACETTEPE UNIVERSITY  
GRADUATE SCHOOL OF SCIENCE AND ENGINEERING  
MASTER THESIS ORIGINALITY REPORT

HACETTEPE UNIVERSITY  
GRADUATE SCHOOL OF SCIENCE AND ENGINEERING  
TO THE DEPARTMENT OF CHEMISTRY

Date: 21/06/2019

Thesis Title: **Interaction of Cibacron Blue Attached Magnetic Polymers with Albumin Using Computational Tools**

According to the originality report obtained by my thesis advisor by using the *Turnitin* plagiarism detection software and by applying the filtering options stated below on 21 / 06 / 2019 for the total of 84 pages including the a) Title Page, b) Introduction, c) Main Chapters, d) Conclusion sections of my thesis entitled as above, the similarity index of my thesis is 9 %.

Filtering options applied:

1. Bibliography excluded
2. Quotes excluded
3. Match size up to 5 words excluded

I declare that I have carefully read Hacettepe University Graduate School of Science and Engineering Guidelines for Obtaining and Using Thesis Originality Reports; that according to the maximum similarity index values specified in the Guidelines, my thesis does not include any form of plagiarism; that in any future detection of possible infringement of the regulations I accept all legal responsibility; and that all the information I have provided is correct to the best of my knowledge.

I respectfully submit this for approval.

21.06.2019  
SEÇKİN KILIÇ

Name Surname: Seçkin Kılıç  
Student No: N16220227  
Department: CHEMISTRY  
Program: CHEMISTRY  
Status:  Masters  Ph.D.  Integrated Ph.D.

**ADVISOR APPROVAL**

  
APPROVED.  
Prof. Dr. Adil Denizli



## CURRICULUM VITAE

Name : Seçkin KILIÇ  
Birthplace : Trabzon  
Birth Date : March 17<sup>th</sup>, 1985  
Mail address : PK345 06443 Yenişehir Ankara  
Phone : +90 (850) 305 3239  
Email : science@seck.in  
Foreign Language : English

## EDUCATION

BSc : Chemistry (Eng.), Hacettepe University.

